

**DIRECT WATER SPLITTING THROUGH HYDROTHERMALLY
SYNTHESIZED BaTiO₃ NANOCRYSTALS**

A DISSERTATION

*Submitted in partial fulfilment of the
requirements for the award of the degree*

of

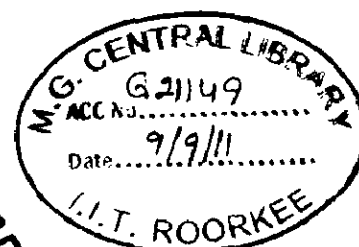
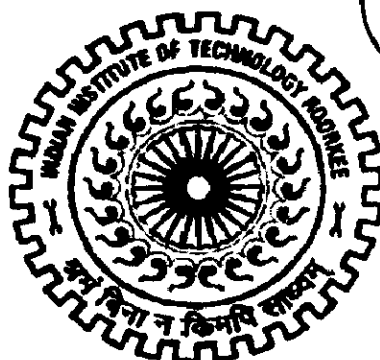
MASTER OF TECHNOLOGY

in

NANOTECHNOLOGY

by

SHASHI KUMAR



**CENTRE OF NANOTECHNOLOGY
INDIAN INSTITUTE OF TECHNOLOGY ROORKEE
ROORKEE-247667 (INDIA)**

JUNE, 2011

CANDIDATE'S DECLARATION

I hereby declare that the work being presented in this dissertation report entitled **“DIRECT WATER SPLITTING THROUGH HYDROTHERMALLY SYNTHESIZED BaTiO₃ NANOCRYSTALS”** for the partial fulfillment of the requirements for the award of the degree of **“Master of technology”** in **“NANOTECHNOLOGY”** is submitted in the Centre of Nanotechnology, Indian Institute of Technology, Roorkee. This report is an authentic record of my own work carried out under the supervision and guidance of **Dr. K.L Yadav**, Associate Professor, Department of Physics, Indian Institute of Technology Roorkee.

The matter embodied in this report work has not been submitted for the award of any other degree.

Date 30 June 2011

Place : Roorkee



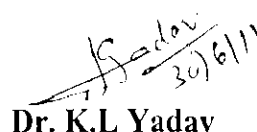
(Shashi Kumar)

CERTIFICATE

This is to certify that the work related to dissertation entitled **“DIRECT WATER SPLITTING THROUGH HYDROTHERMALLY SYNTHESIZED BaTiO₃ NANOCRYSTALS”** has been carried out by **Mr. Shashi Kumar** under my supervision for the partial fulfillment of **“Master of Technology”** with specialization in **“Nanotechnology”**.

Date:

Place: Roorkee



Dr. K.L Yadav

Associate Professor,
Department of Physics
Indian Institute of Technology
Roorkee-247667, India

ACKNOWLEDGMENTS

First and foremost, I would like to express my sincere gratitude to my supervisor, **Dr. K.L Yadav**, who supported throughout my M.Tech Dissertation with his guidance, motivation, encouragement and immense knowledge. He always provide me enough freedom and resources to work in my own way. His meticulous guidance and precious suggestions played a vital source of inspiration for bringing the present work in final form. One simply couldn't wish for a better or friendlier supervisor.

I am thankful to **Prof. Anil kumar**, Head of Center of Nanotechnology, for providing me the necessary facilities to complete this dissertation work.

I am deeply indebted to Dr. Ramesh Chandra, Institute Instrumentation Center, IIT Roorkee, who has allowed me to use the facilities of his lab and of Institute Instrumentation Center necessary for the completion of this dissertation work.

My Gratitude also goes to all my friends and colleagues Kirandeep Singh, Azad Yadav, Deepesh Yadav, Ajit Singh, Kunal Shridhar, Gaurav Shukla, Chanchal Yevale, Naman Varshney and Jhonson Khakha who supported me by giving their valuable suggestions. I thank them all for their full co-operation and for also being around all time. I wish to acknowledge Mr. Abdul Haq, Lab Assistant in our lab for his affection and cooperation.

The financial help provided by MHRD, Govt. Of India is gratefully acknowledge.

I have no words to express appreciation to my family for their understanding and support during all these years. I could not have reached this important milestone of my life without their support and encouragement.

And above all, I am thankful to the Almighty whose divine grace gave me the enough courage, strength and perseverance to overcome various obstacles that stood in my way.

(Shashi Kumar)

LIST OF FIGURES

- Figure 1.1** Schematic diagram of dipole moment
- Figure 1.2** Condition for the existence of dipole moment
- Figure 1.3** Six possible directions for the alignment of dipole moment
- Figure 1.4** Cross sectional view of the alignment of domains in a cubic system
- Figure 1.5** Relation between piezoelectrics, pyroelectrics and ferroelectrics
- Figure 1.6(a, b, c, d)** Relation between pyroelectrics and ferroelectrics with curie temperature
- Figure 1.7** Ferroelectric multiple domain
- Figure 1.8** Ferroelectric domains under electric field
- Figure 1.9** Effect of mechanical stress on domains
- Figure 1.10** A piezoelectric disk generates a voltage when deformed
- Figure 1.11** Polar crystals
- Figure 1.12** Schematic diagram of perovskite structure
- Figure 1.13** BaTiO₃ structure
- Figure 1.14** Effect of temperature on BaTiO₃ structure
- Figure 1.15** BaTiO₃ structures at different temperatures
- Figure 2.1** Schematic diagram of the sample preparation
- Figure 2.2** Parameters affecting the size of the crystal formed
- Figure 2.3 (a, b, c)** Diagram shows the physics and chemistry of the reaction
- Figure 2.4** Hydrogen production vs. Time duration
- Figure 2.5** PZEC efficiency vs. fiber length
- Figure 3.1** Schematic diagram of beam path.
- Figure 3.2** Photograph of Bruker D8 Advance X-ray Diffractometer
- Figure 3.3** Specimen beam interaction.
- Figure 3.4** Quanta 200F FEI model of Field emission scanning electron microscope

LIST OF FIGURES

- Figure 3.5** Schematic diagram of FESEM
- Figure 3.6** Equipments used for hydrothermal synthesis process
- Figure 3.7** Vacuum pump
- Figure 3.8** Characteristic set up of a laboratory vacuum filtration
- Figure 3.9** Ultrasonic cleaner
- Figure 3.10** Set up of Gas chromatography
- Figure 3.11** Line diagram of Gas Chromatography
- Figure 4.1** Equipments used for hydrothermal process
- Figure 4.2** Complete layout of the hydrothermal process for BaTiO₃
- Figure 5.1** Equipments used for the water splitting purposes
- Figure 5.2(a, b, c, d, e, f)** Layout of complete water splitting process and gas detection technique
- Figure 6.1** XRD image for BaTiO₃ samples S₁, S₂ and S₃
- Figure 6.2** FE-SEM images of BaTiO₃ samples S₁, S₂ and S₃ respectively
- Figure 7.1** Future application in the field of automobiles – Self-hydrogen generation vehicles
- Figure 7.2** Detail descriptions of some parts of Self-hydrogen generation vehicles

LIST OF TABLES

- Table 1.1** Properties of BaTiO₃ Perovskite structure
- Table 3.1** Technical specifications of the vacuum pump
- Table 4.1** Parameters used for the synthesis of BaTiO₃ Sample (S₁)
- Table 4.2** Parameters used for the synthesis of BaTiO₃ Sample (S₂)
- Table 4.3** Parameters used for the synthesis of BaTiO₃ Sample (S₃)
- Table 6.1** XRD data for BaTiO₃ samples S₁, S₂ and S₃
- Table 6.2** Fibre length of BaTiO₃ samples S₁, S₂ and S₃

CANDIDATE'S DECLARATION	i
CERTIFICATE	i
ACKNOWLEDGMENTS	ii
LIST OF FIGURE	iii
LIST OF TABLES	v
CONTENTS	vi

CHAPTER – 1 INTRODUCTION 1 - 21

1.1 Ferroelectric	
1.1.1 Spontaneously polarized piezoelectrics	
1.2 Piezoelectricity	
1.2.1 Mechanism	
1.2.2 Mathematical description	
1.2.3 Crystal classes	
1.3 Perovskite structure	
1.4 BaTiO₃	
References	

CHAPTER – 2 LITERATURE REVIEW 22 - 34

2.1 Synthesis	
2.2 Analysis	
2.3 Characterization	
2.4 Water splitting process	
2.5 PZEC efficiency calculation	
References	

Chapter 3 – EXPERIMENTAL TECHNIQUE 35 - 63

3.1 Basic structural characterization techniques	
3.1.1 X-ray diffraction (XRD)	
3.1.2 Field emission scanning electron microscopy (FE-SEM)	
3.2 Hydrothermal synthesis	
3.2.1 Volumetric flask	

- 3.2.2 Teflon (PTFE) container
- 3.2.3 Stainless steel autoclave
- 3.2.4 Electric furnace
- 3.3 Water splitting process
 - 3.3.1 Vacuum pump
 - 3.3.2 Ultrasonic cleaner
- 3.4 Hydrogen gas detection technique
 - 3.4.1 Gas chromatography
- References

Chapter 4 – HYDROTHERMAL SYNTHESIS AND CHARACTERIZATION OF NANO CRYSTALS 64-78

- 4.1 Hydrothermal synthesis
 - 4.1.1 Equipments for hydrothermal crystal growth
- 4.2 Experimental details
 - 4.2.1 Data and formula needed for calculating the amount of chemicals
 - 4.2.2 Sample (S₁)
 - 4.2.3 Sample (S₂)
 - 4.2.4 Sample (S₃)
- References

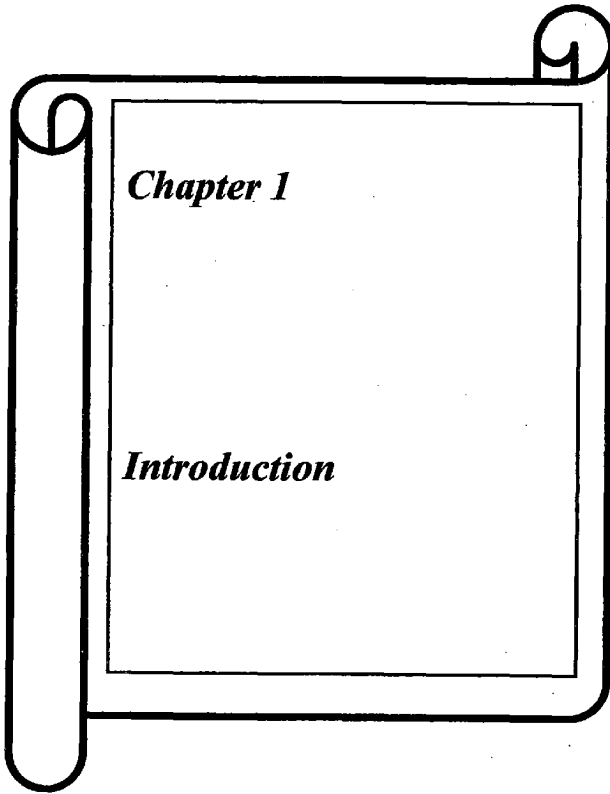
Chapter 5 – Direct water splitting through Nano crystals 79-91

- 5.1 Water splitting
- 5.2 Experimental details
- References

Chapter 6 – Results and Conclusions 92-94

- 6.1 XRD data
- 6.2 FE-SEM data
- References

Chapter 7 – Future Prospects 95-97



Chapter 1

Introduction

1.1 Ferroelectric

The ferroelectric effect [1] was first observed by Valasek in 1921, in the Rochelle salt. This has molecular formula $\text{KNaC}_4\text{H}_4\text{O}_6 \cdot 4\text{H}_2\text{O}$. The effect was then not considered for some time, and it wasn't until a few decades ago that they came into great use. Nowadays, ferroelectric materials are used widely, mainly in memory applications

To be ferroelectric, a material must possess a spontaneous dipole moment that can be switched in an applied electric field, i.e. spontaneous switchable polarisation. This is found when two particles of charge q are separated by some distance r , i.e.:

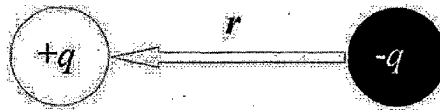


Figure 1.1 Schematic diagram of dipole moment

The dipole moment, μ is:

$$\mu = q \cdot r$$

In a ferroelectric material [2], there is a net permanent dipole moment, which comes from the vector sum of dipole moments in each unit cell, $\Sigma\mu$. This means that it cannot exist in a structure that has a centre of symmetry, as any dipole moment generated in one direction would be forced by symmetry to be zero. Therefore, ferroelectrics must be non-centrosymmetric. This is not the only requirement however. There must also be a spontaneous local dipole moment (which typically leads to a macroscopic polarisation, but not necessarily if there are domains that cancel completely). This means that the central atom

must be in a non-equilibrium position. For example, consider an atom in a tetrahedral interstice.

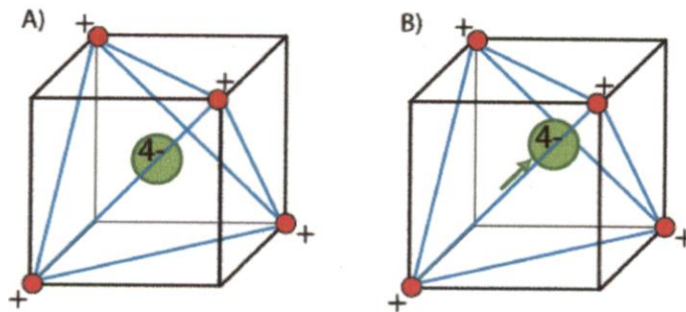


Figure 1.2 Condition for the existence of dipole moment

In (A) the structure is said to be non-polar. There is no displacement of the central atom, and no net dipole moment. In (B) however, the central atom is displaced and the structure is polar. There is now an inherent dipole moment in the structure. This results in a polarisation. Polarisation may be defined as the total dipole moment per unit volume, i.e.

$$P = \frac{\sum \mu}{V}$$

Materials are polarised along a unique crystallographic direction, in that certain atoms are displaced along this axis, leading to a dipole moment along it. Depending on the crystal system, there may be few or many possible axes. As it is the most common and easy to see, let us examine a tetragonal system that forms when cooled from the high temperature cubic phase, through the Curie temperature, of e.g. $T_c = 120^\circ\text{C}$ in BaTiO_3 .

In this system, the dipole moment can lie in 6 possible directions corresponding to the original cubic axes:

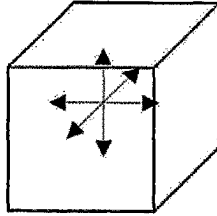


Figure 1.3 Six possible directions for the alignment of dipole moment

In a crystal, it is likely that dipole moments of the unit cells in one region lie along a different one of the six directions to the dipole moments in another region. Each of these regions is called a domain, and a cross section through a crystal can look like this:

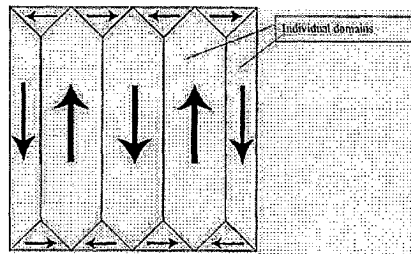


Figure 1.4 Cross sectional view of the alignment of domains in a cubic system

A domain is a homogenous region of a ferroelectric, in which all of the dipole moments in adjacent unit cells have the same orientation. In a newly-grown single crystal, there will be many domains, with individual polarisations such that there is no overall polarisation. The polarisation of individual domains is organised such that +ve heads are held near -ve tails. This leads to a reduction in stray field energy, because there are fewer isolated heads and tails of domains. This is analogous to the strain energy reduction found in dislocation stacking.

Domain boundaries are arranged so that the dipole moments of individual domains meet at either 90° or 180° . In a polycrystal (one with more than one crystallographic grain), the

arrangement of domains depends on grain size. If the grains are fine ($\ll 1$ micron), then there is usually found to be one domain per grain. In larger grains there can be more than one domain in each grain.

In an electric field, E , a polarised material lowers its energy by $-P.E$, (where P is the polarisation). Any dipole moments which lie parallel to the electric field are lowered in energy, while moments that lie perpendicular to the field are higher in energy and moments that lie anti-parallel are even higher in energy, $(+P.E)$.

This introduces a driving force to minimise the free energy, such that all dipole moments align with the electric field.

1.1.1 Spontaneously polarized piezoelectrics

Ferroelectrics are spontaneously polarised [3], but are also piezoelectric, in that their polarisation changes under the influence of a stress. This is because while all ferroelectrics are piezoelectric, not all piezoelectrics are ferroelectric. This relationship [4] can be viewed as:

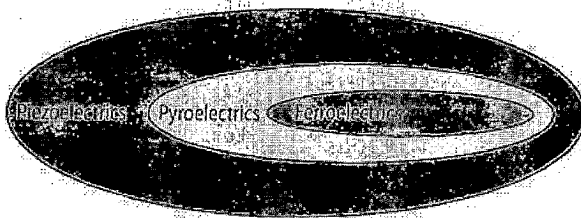
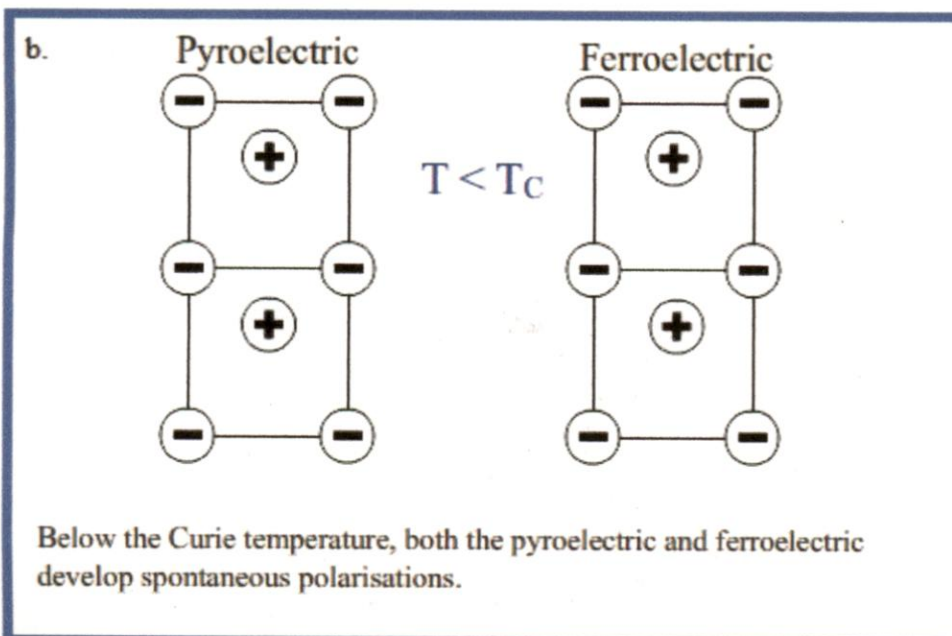
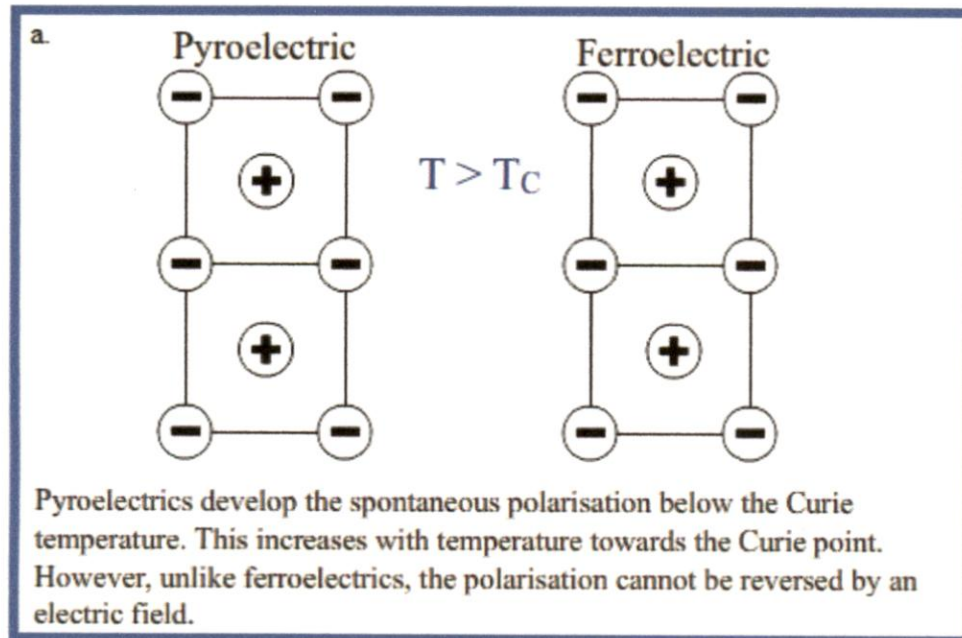


Figure 1.5 Relation between piezoelectrics, pyroelectrics and ferroelectrics

Pyroelectrics are materials which typically experience a decrease in polarisation when their temperature is increased. Pyroelectrics are the bridge between ferroelectrics and

piezoelectrics. They possess a spontaneous polarisation which is not necessarily switchable by an electric field. If their polarisation is electrically switchable then they are ferroelectric.



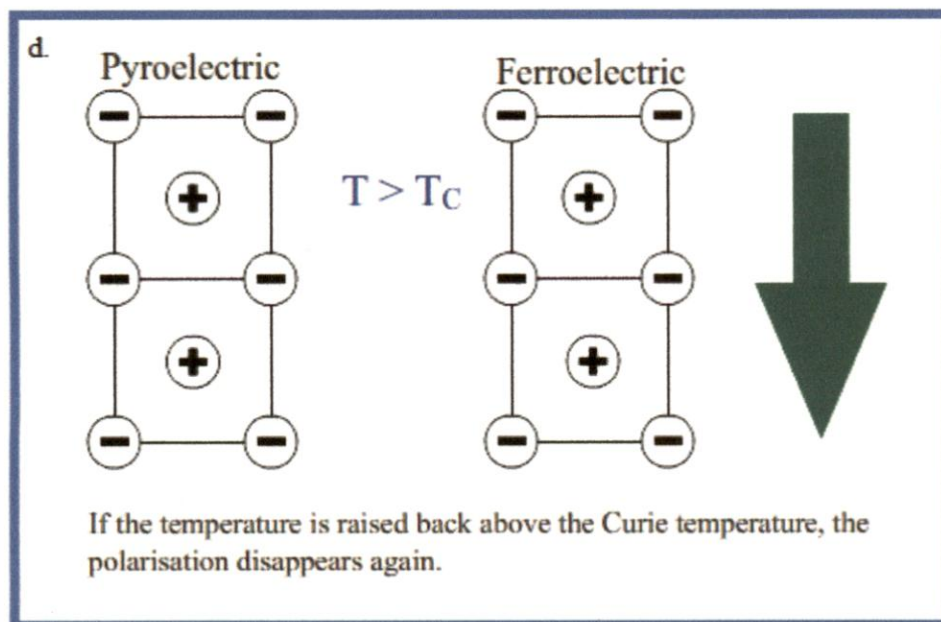
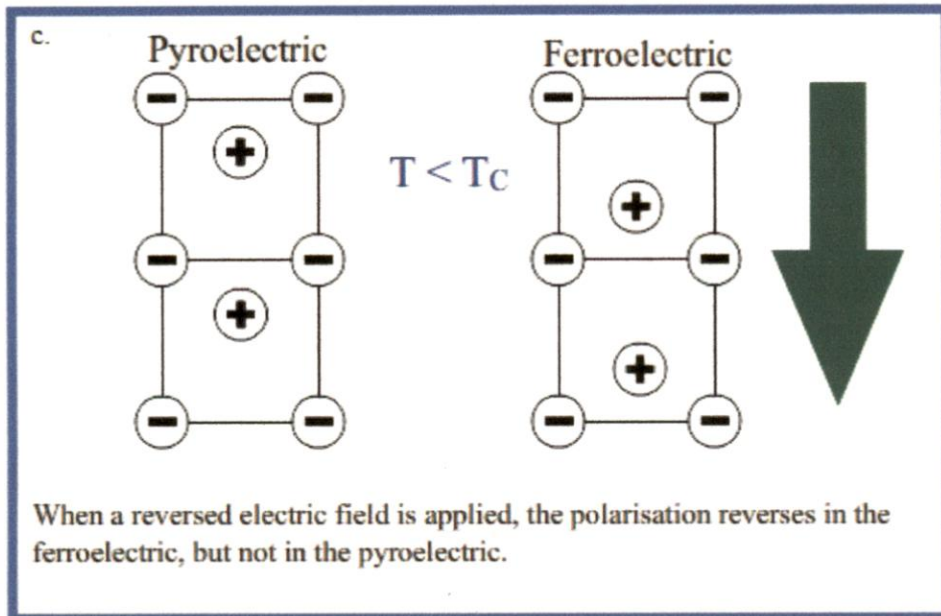


Figure 1.6 (a, b, c, d) Relation between pyroelectrics and ferroelectrics with curie temperature

Ferroelectric materials possess multiple domains. To make it simple, we will only consider

single crystal ferroelectrics. These, when first made, have domains of the form:

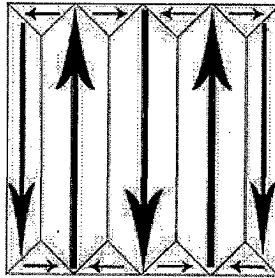


Figure 1.7 Ferroelectric multiple domain

If a mechanical stress is applied to the ferroelectric, then there are domains which will experience an increase in dipole moment and some which will experience a decrease in dipole moment. Overall, there is no net increase in polarisation. This makes BaTiO_3 useless as a piezoelectric unless it is put through some additional processing. This process is called *poling*. An electric field is applied to the ferroelectric as it passes through its Curie temperature, so as its spontaneous polarisation develops, it is aligned in a single direction:

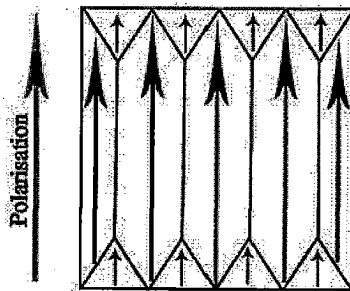
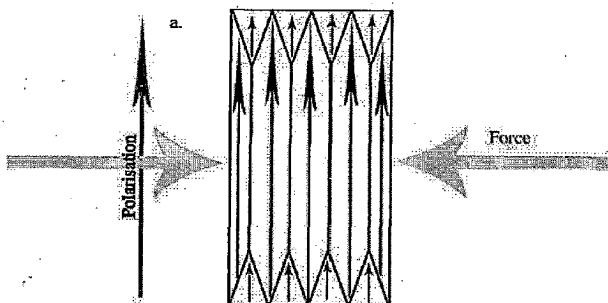


Figure 1.8 Ferroelectric domains under electric field

All of the domains in the piezoelectric have a dipole moment pointing in the same

direction, so there is a net spontaneous polarisation. Now, when a mechanical stress is applied, the polarisation will

increase:



or decrease:

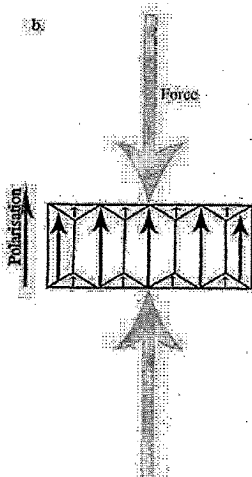


Figure 1.9 Effect of mechanical stress on domains

but still remain pointing in the original direction. This makes ferroelectrics into useful piezoelectrics.

1.2 Piezoelectricity

Piezoelectricity [5] is the charge which accumulates in certain solid materials (notably crystals, certain ceramics, and biological matter) in response to applied mechanical stress. The word *piezoelectricity* means electricity resulting from pressure. It is derived from the Greek *piezo* which means to squeeze or press, and *electric* which stands for amber, an ancient source of electric charge. Piezoelectricity is the direct result of the piezoelectric effect.

The piezoelectric effect is understood as the linear electromechanical interaction between the mechanical and the electrical state in crystalline materials with no inversion symmetry.^[3] The piezoelectric effect is a reversible process in that materials exhibiting the direct piezoelectric effect (the internal generation of electrical charge resulting from an applied mechanical force) also exhibit the reverse piezoelectric effect (the internal generation of a mechanical force resulting from an applied electrical field).

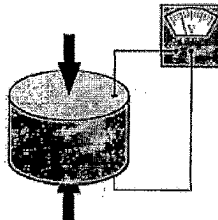


Figure 1.10 A piezoelectric disk generates a voltage when deformed

1.2.1 Mechanism

The nature of the piezoelectric effect is closely related to the occurrence of electric dipole moments in solids. The latter may either be induced for ions on crystal lattice sites with asymmetric charge surroundings (as in BaTiO_3 and PZTs) or may directly be carried by molecular groups (as in cane sugar). The dipole density or polarization (dimensionality [Cm/m^3]) may easily be calculated for crystals by summing up the dipole moments per volume of the crystallographic unit cell. As every dipole is a vector, the dipole density \mathbf{P} is also a vector or a directed quantity. Dipoles near each other tend to be aligned in regions called Weiss domains. The domains are usually randomly oriented, but can be aligned using the process of *poling* (not the same as magnetic poling), a process by which a strong electric field is applied across the material, usually at elevated temperatures. Not all piezoelectric materials can be poled.

Of decisive importance for the piezoelectric effect is the change of polarization \mathbf{P} when applying a mechanical stress. This might either be caused by a re-configuration of the dipole-inducing surrounding or by re-orientation of molecular dipole moments under the influence of the external stress. Piezoelectricity may then manifest in a variation of the polarization strength, its direction or both, with the details depending on 1. the orientation of \mathbf{P} within the crystal, 2. Crystal symmetry and 3. the applied mechanical stress. The change in \mathbf{P} appears as a variation of surface charge density upon the crystal faces, i.e. as a variation of the electrical field extending between the faces, since the units of surface charge density and polarization are the same. However, piezoelectricity is not caused by a change in charge density on the surface, but by dipole density in the bulk. Piezoelectric materials also show the opposite effect, called *converse piezoelectric effect*, where the application of an electrical field creates mechanical deformation in the crystal.

1.2.2 Mathematical description

Piezoelectricity is the combined effect of the electrical behaviour of the material:

$$D = \epsilon E$$

where D is the electric charge density displacement (electric displacement), ϵ is permittivity and E is electric field strength,

and

Hooke's Law:

$$S = sT$$

where S is strain, s is compliance and T is stress.

1.2.3 Crystal classes

Any spatially separated charge will result in an electric field, and therefore an electric potential. Shown here is a standard dielectric in a capacitor. In a piezoelectric device, mechanical stress, instead of an externally applied voltage, causes the charge separation in the individual atoms of the material, the polar crystal classes, which show a spontaneous polarization without mechanical stress due to a non-vanishing electric dipole moment associated with their unit cell, and which exhibit pyroelectricity. If the dipole moment can be reversed by the application of an electric field, the material is said to be ferroelectric.

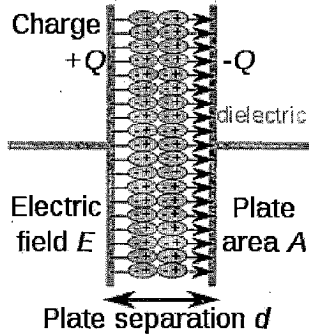


Figure 1.11 Polar crystals

For polar crystals, for which $\mathbf{P} \neq 0$ holds without applying a mechanical load, the piezoelectric effect manifests itself by changing the magnitude or the direction of \mathbf{P} or both. For the non-polar, but piezoelectric crystals, on the other hand, a polarization \mathbf{P} different from zero is only elicited by applying a mechanical load. For them the stress can be imagined to transform the material from a non-polar crystal class ($\mathbf{P} = 0$) to a polar one,^[5] having $\mathbf{P} \neq 0$.

1.3 Perovskite Structure

A perovskite structure [6] is any material with the same type of crystal structure as calcium titanium oxide (CaTiO_3), known as the perovskite structure, or $\text{XII A}^{2+\text{VI}}\text{B}^{4+\text{X}2-}_3$ with the oxygen in the face centers.^[2] Perovskites take their name from this compound, which was first discovered in the Ural mountains of Russia by Gustav Rose in 1839 and is named after Russian mineralogist L. A. Perovski (1792–1856). The general chemical formula for perovskite compounds is ABX_3 , where 'A' and 'B' are two cations of very different sizes, and X is an anion that bonds to both. The 'A' atoms are larger than the 'B' atoms. The ideal cubic-symmetry structure has the B cation in 6-fold coordination, surrounded by an

octahedron of anions, and the A cation in 12-fold cuboctahedral coordination. The perovskite structure is adopted by many oxides that have the chemical formula ABO_3 . In the idealized cubic unit cell of such a compound, type 'A' atom sits at cube corner positions (0, 0, 0), type 'B' atom sits at body centre position (1/2, 1/2, 1/2) and oxygen atoms sit at face centred positions (1/2, 1/2, 0). (The diagram shows edges for an equivalent unit cell with B at the corners, A in body centre, and O in mid-edge). The A cations may be monovalent or bivalent, B cations may be tetravalent or pentavalent.

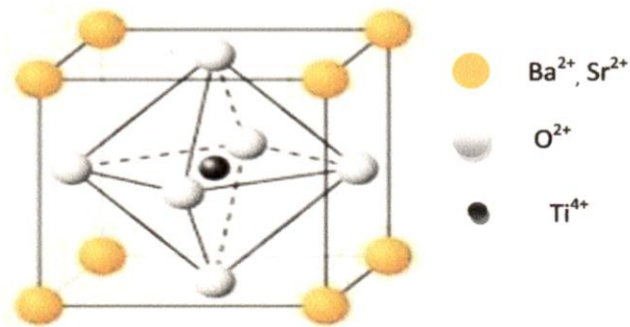


Figure 1.12 Schematic diagram of perovskite structure

1.4 $BaTiO_3$

Most of the important ferroelectrics are oxides that possess the well-known perovskite structure. $BaTiO_3$ [7] is one such potential oxide having a perovskite structure. Besides its outstanding properties with respect to piezoelectricity, pyroelectricity, and high dielectric constant, $BaTiO_3$ shows ferroelectricity at room temperature. For $BaTiO_3$, Ti is a 3d transition element and has the d orbital for electrons to form covalent bonds with its neighbors. The radius of Ti^{4+} ion is about 0.68 Å, and that of Ba^{2+} is about 1.35 Å. These ions form nice octahedral cages, with the O^{2-} ions held apart. The structure of $BaTiO_3$ is temperature dependent at a certain transition temperature, the particular structure of the unit

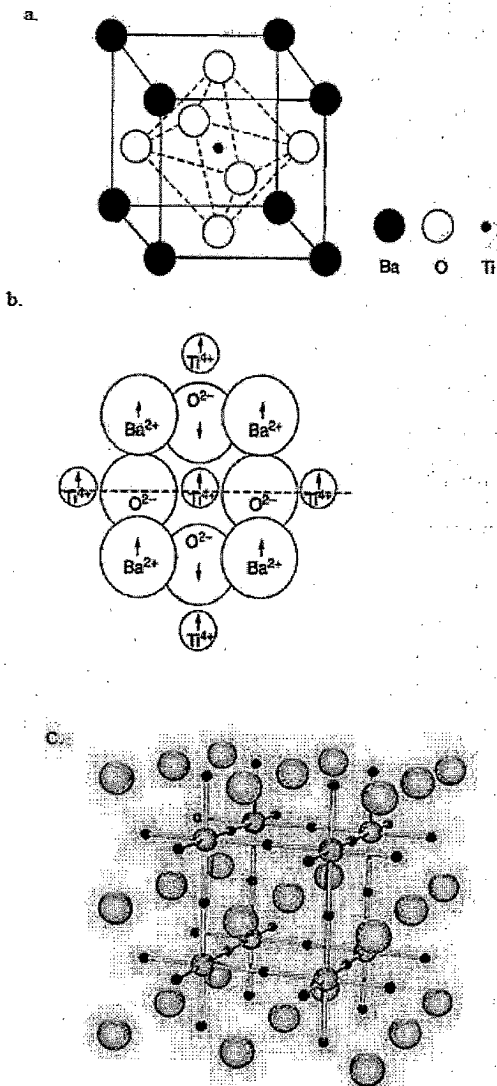
cell becomes unstable and must transform to a more stable one. The temperature dependence of BaTiO_3 structure is shown in fig (). Below 120°C the structure changes from cubic to tetragonal resulting from the stretching of the cubic unit cells along one edge, as shown in Figure. In fact, the Ba^{2+} ions shift upward from their original position in the cubic structure; Ti^{4+} ions shift upward, and the O_2^- ions downward to form the tetragonal structure. As a result of the ion shifts, the centroid of the positive charges no longer coincides with the centroid of the negative charges; therefore, the unit cells become permanently polarized and behave as permanent dipoles, leading to spontaneous polarization.

1.4.1 Properties

The solid can exist in five phases, listing from high temperature to low temperature: hexagonal, cubic, tetragonal, orthorhombic, and rhombohedral crystal structure. All of the phases exhibit the ferroelectric effect except the cubic phase. The high temperature cubic phase is easiest to describe, consisting of octahedral TiO_6 centres that define a cube with Ti vertices and Ti-O-Ti edges. In the cubic phase, Ba^{2+} is located at the centre of the cube, with a nominal coordination number of 12. Lower symmetry phases are stabilized at lower temperatures, associated with the movement of the Ba^{2+} to off-centre position. The remarkable properties of this material arise from the cooperative behaviour of the Ba^{2+} centres.

Molecular mass	233.192g/mol
Appearance	White crystal
Density	6.02g/cm ³ , solid
Melting point	1625 ^o C
Solubility in water	Insoluble

Table 1.1 Properties of BaTiO_3 Perovskite structure

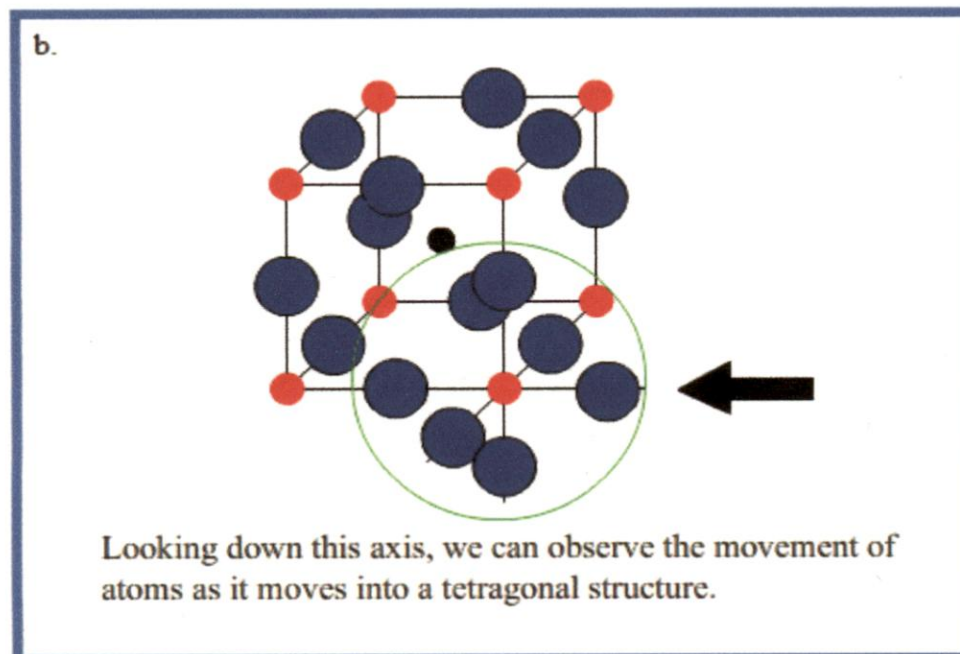
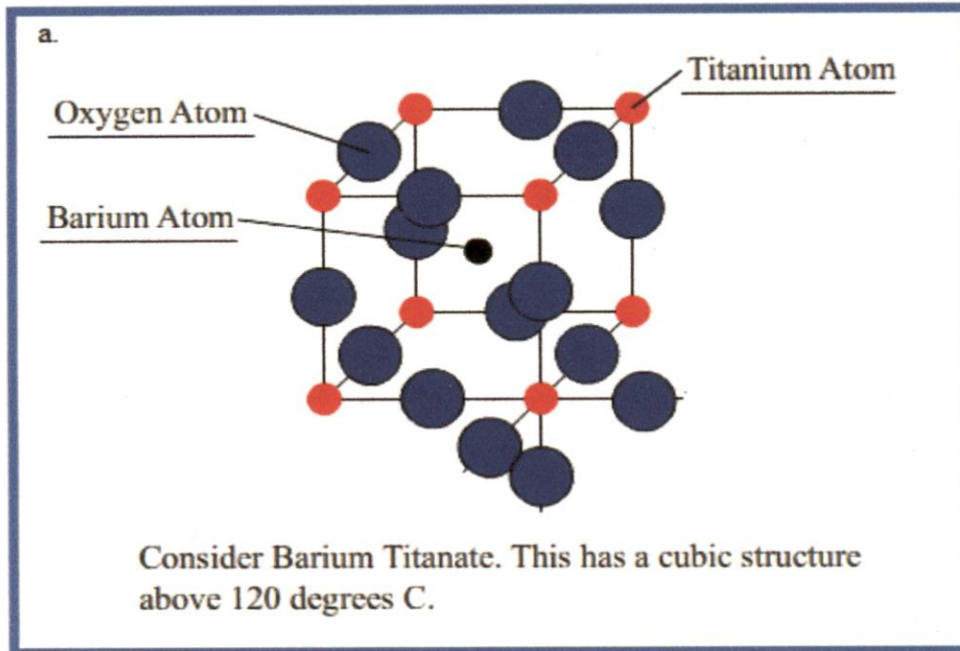
Figure 1.13 BaTiO₃ structure

1.4.2 Curie Temperature

In analogy to ferroelectric materials, the Curie temperature is used in piezoelectric materials to describe the temperature above which the material loses its spontaneous polarization and piezoelectric characteristics.

The Curie temperature [T_C] for BaTiO_3 is 120°C .

- $T > T_C$: - Cubic Structure - It is centro-symmetric and possesses no spontaneous dipole. With no dipole the material behaves like a simple dielectric, giving a linear polarisation. .
- $T < T_C$: - Tetragonal phase - Cooling through T_C causes the cubic phase to transform to a tetragonal phase with the lengthening of the c lattice parameter (and a corresponding reduction in a and b).



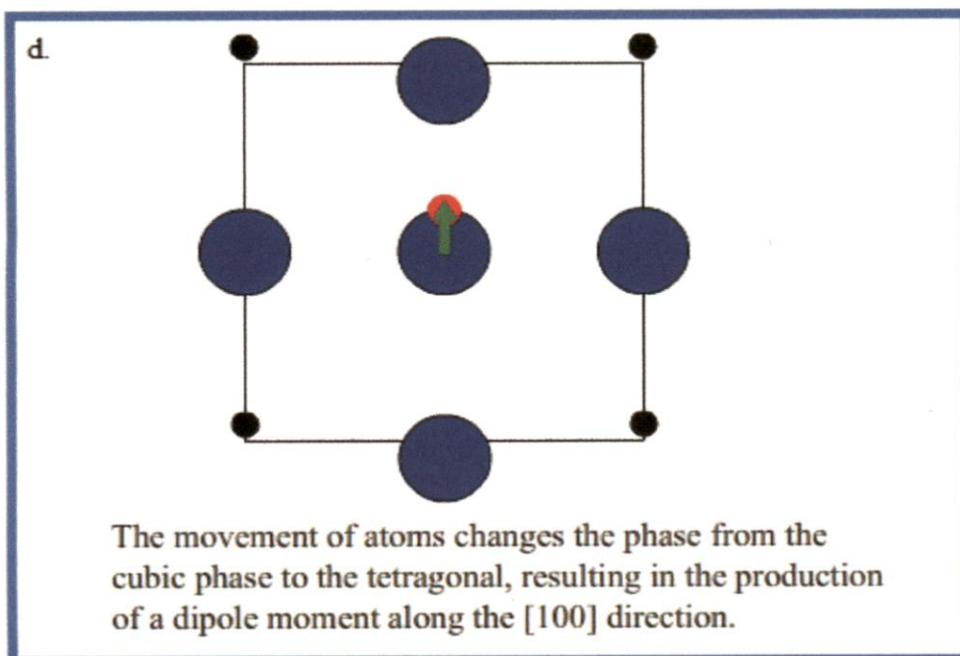
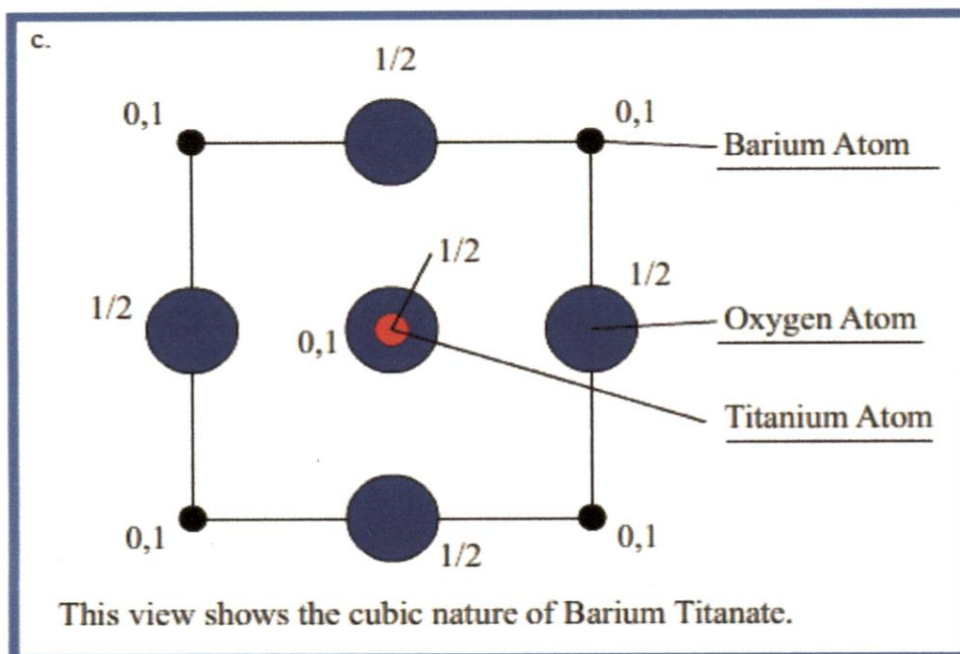
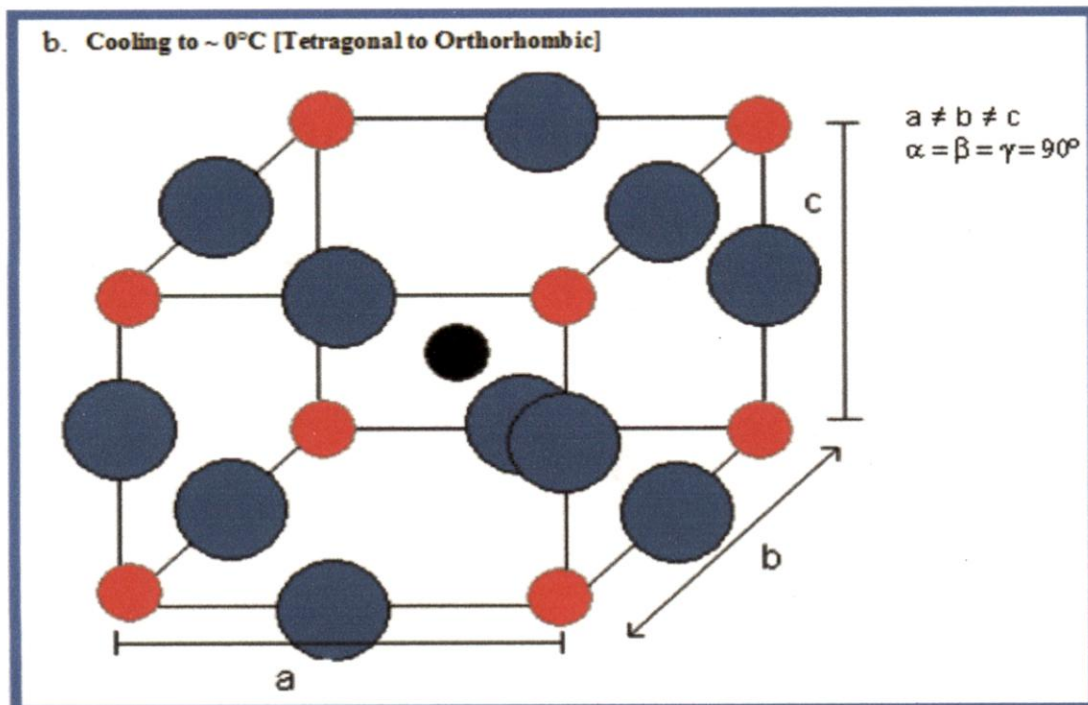
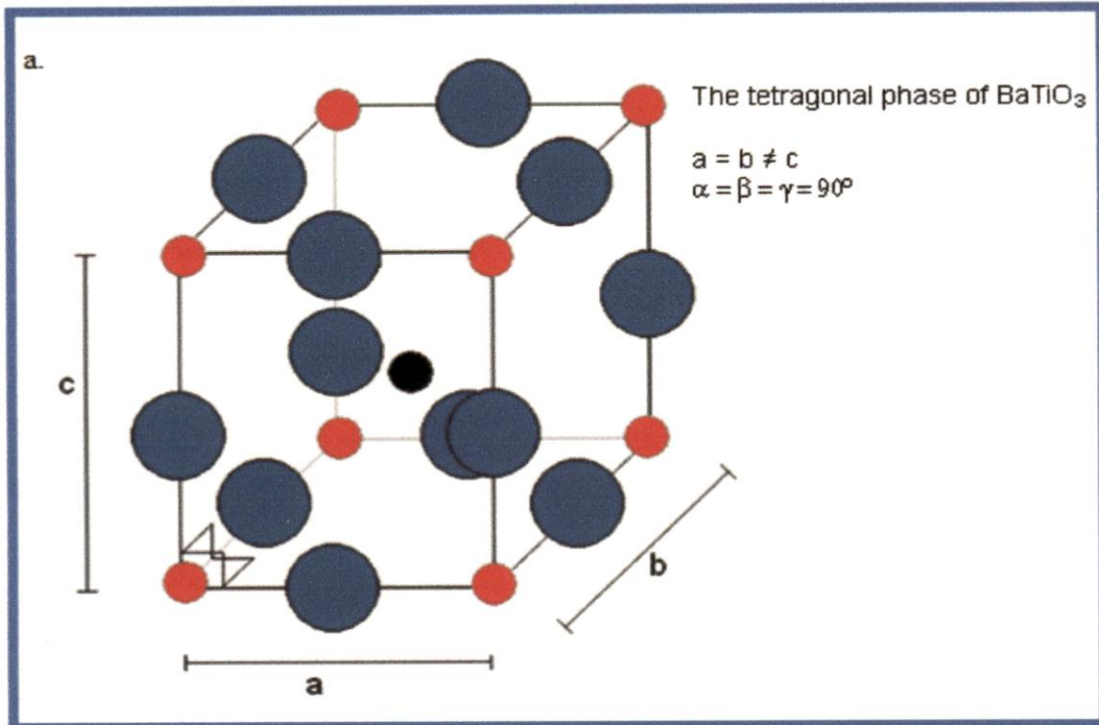


Figure 1.14 Effect of temperature on BaTiO₃ structure



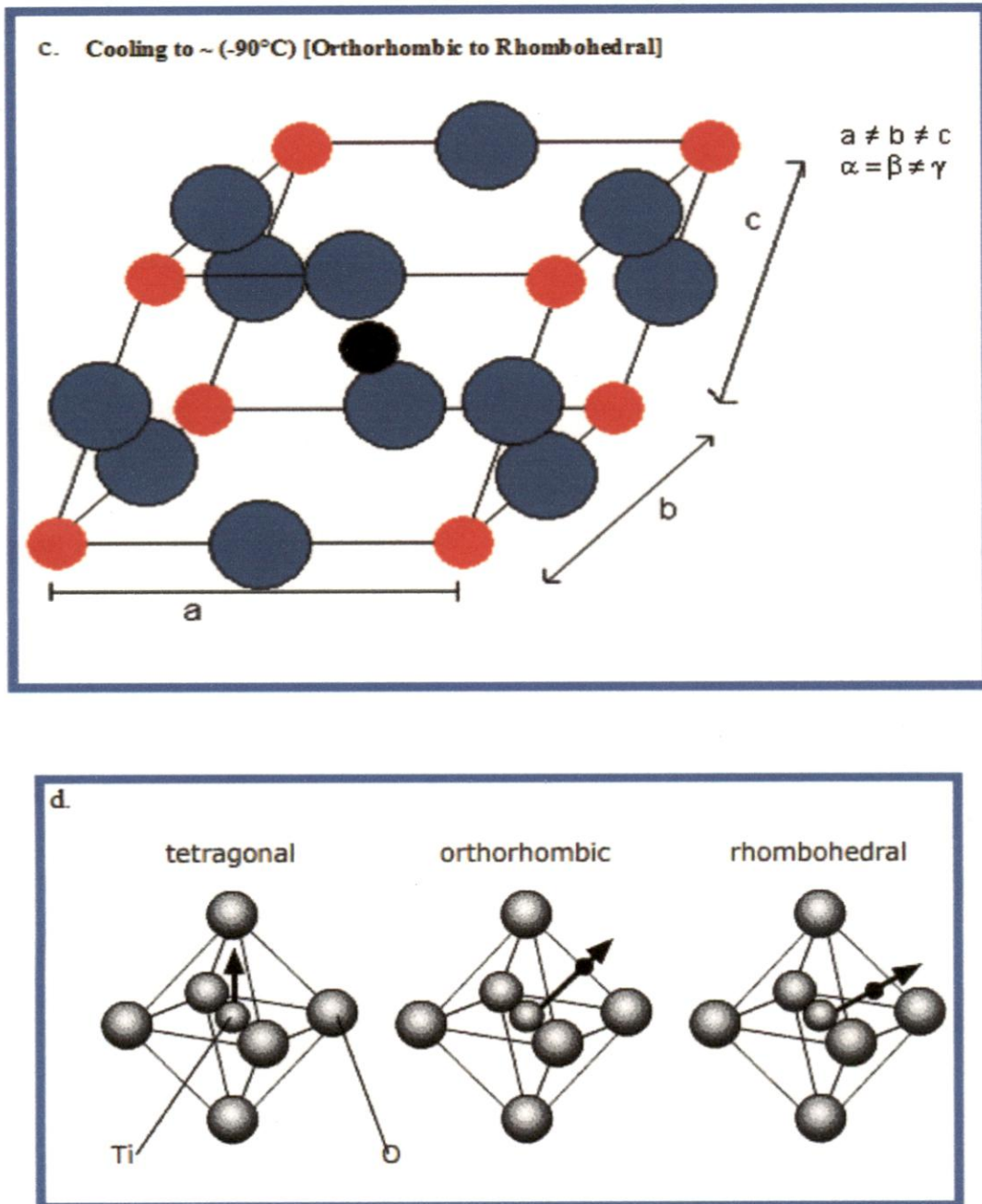
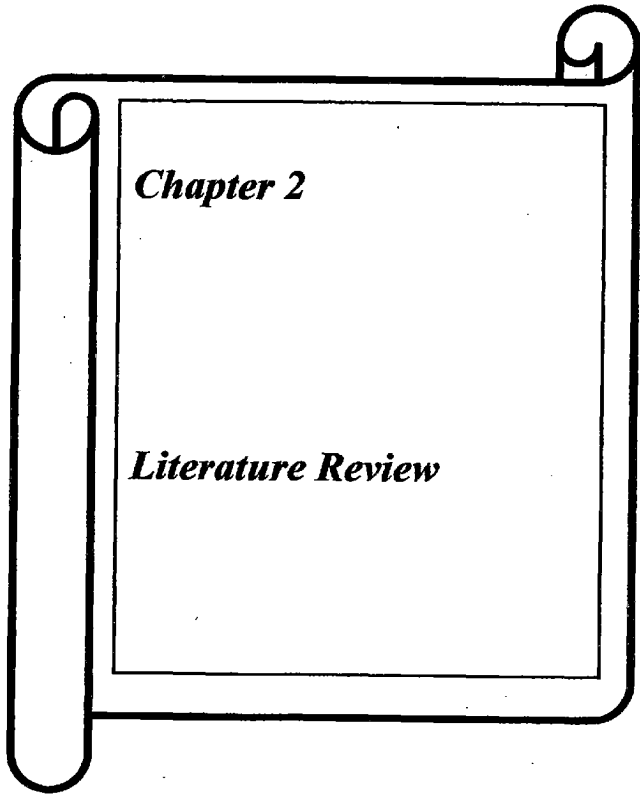


Figure 1.15 BaTiO_3 structures at different temperatures

References

- [1] A. S. Sidorkin (2006). Domain Structure in Ferroelectrics and Related Materials. Cambridge University Press.
- [2] Karin M Rabe, Jean-Marc Triscone, Charles H Ahn (2007). Physics of Ferroelectrics: A modern perspective. Springer.
- [3] Land g, Sidney B., 2005, "Pyroelectricity: From Ancient Curiosity to Modern Imaging Tool," Physics Today, Vol 58, p.31
- [4] Gautschi, Gustav, 2002, Piezoelectric Sensorics, Springer,
- [5] Damjanovic, Dragan (1998). "Ferroelectric, dielectric and piezoelectric properties of ferroelectric thin films and ceramics". Reports on Progress in Physics **61**: 1267–1324
- [6] Wenk, Hans-Rudolf; Bulakh, Andrei (2004). Minerals: Their Constitution and Origin. New York, NY: Cambridge University Press
- [7] Nyutu, Edward K.; Chen, Chun-Hu; Dutta, Prabir K.; Suib, Steven L. (2008). "Effect of Microwave Frequency on Hydrothermal Synthesis of Nanocrystalline Tetragonal Barium Titanate". The Journal of Physical Chemistry C **112**: 9659.



Chapter 2

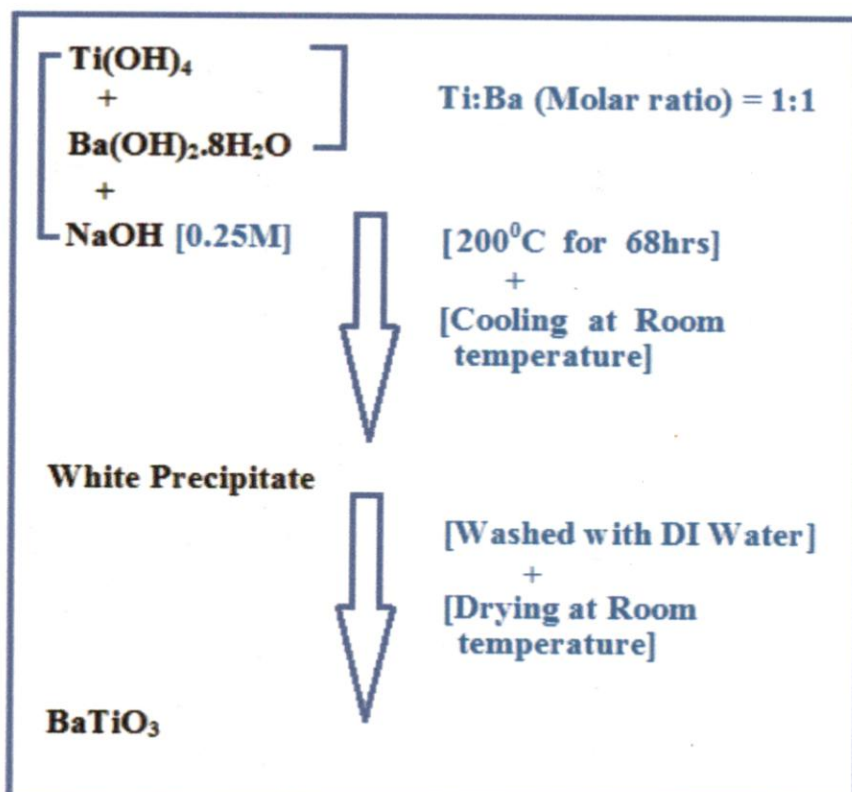
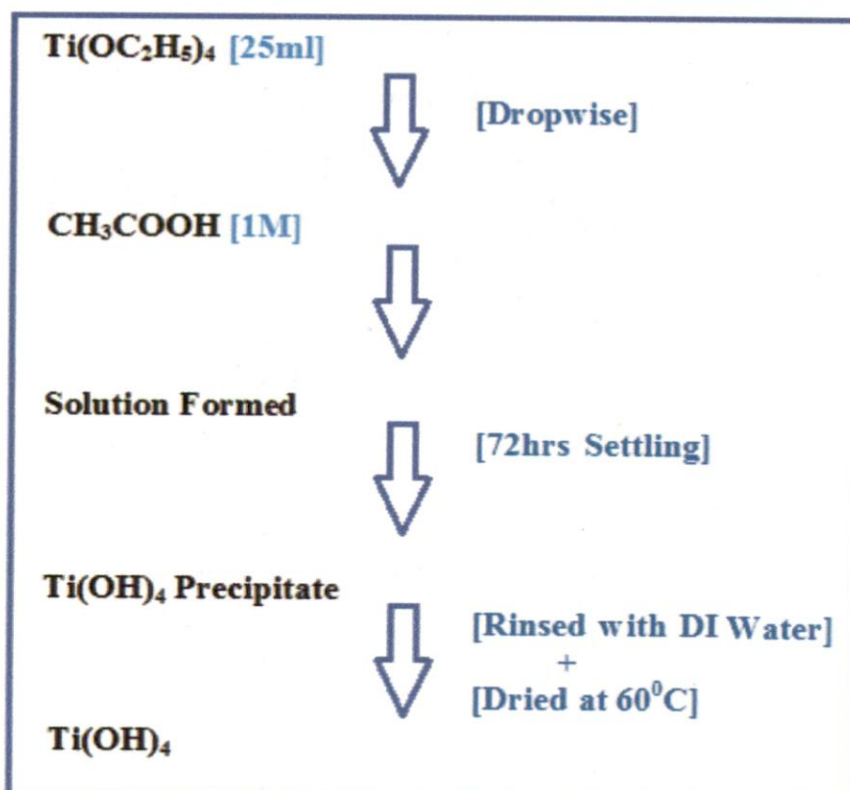
Literature Review

2.1 Synthesis

A piezoelectrochemical effect for the direct conversion of mechanical energy to chemical energy is the basic mechanism of the work. This phenomenon is further applied for generating hydrogen and oxygen via direct water decomposition by means of as-synthesized piezoelectric BaTiO₃ micro-dendrites. Dendrites are vibrated with ultrasonic waves leading to a strain-induced electric charge development on their surface. With sufficient electric potential, strained piezoelectric dendrites in water triggered the redox reaction of water to produce hydrogen and oxygen gases. BaTiO₃ micro-dendrites under ultrasonic vibrations [1] showed a stoichiometric ratio of H₂/O₂ (2:1) initial gas production from pure water.

The BaTiO₃ dendrite samples of the PZEC catalyst [2] were synthesized by a hydrothermal method. All of the chemicals that were used as starting materials had a purity of 99.99%. The precursor Ti(OH)₄ was prepared by adding 25ml of Ti(OC₂H₅)₄ dropwise into 1.0 M acetic acid. The solution was settled, allowing the precipitate to form in 72 h, and followed by rinsing of the product with DI water and drying at 60°C. The as-synthesized Ti(OH)₄ precursor and commercially available Ba(OH)₂·8H₂O were then added (Ti/Ba = 1:1 in molar ratio) into 0.25 M NaOH. After that, the mixture in a Teflon cup with 60% capacity was stirred and sealed tightly in a stainless steel autoclave. The closed bomb (Parr-type) [3] was maintained at 200°C for 68 h for hydrothermal reaction. The bomb was then cooled naturally to room temperature. The resulting white precipitate was washed extensively with DI water to remove any adsorbed impurities and finally dried at room temperature. The acetic acid (CH₃COOH) acts as a chelating ligand in the reaction mechanism and performs the following function

- It inhibits the quick hydrolysis of the precursor
- It decreases the rate of condensation to allow more linear polycondensation of the precursor, leading to fine, more homogeneous particles of the precipitate.



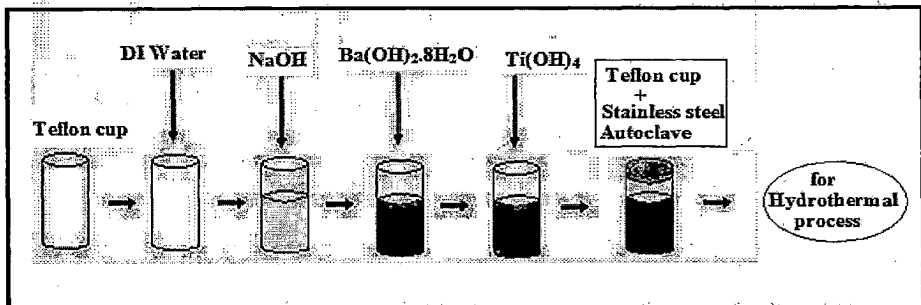


Figure 2.1 Schematic diagram of the sample preparation

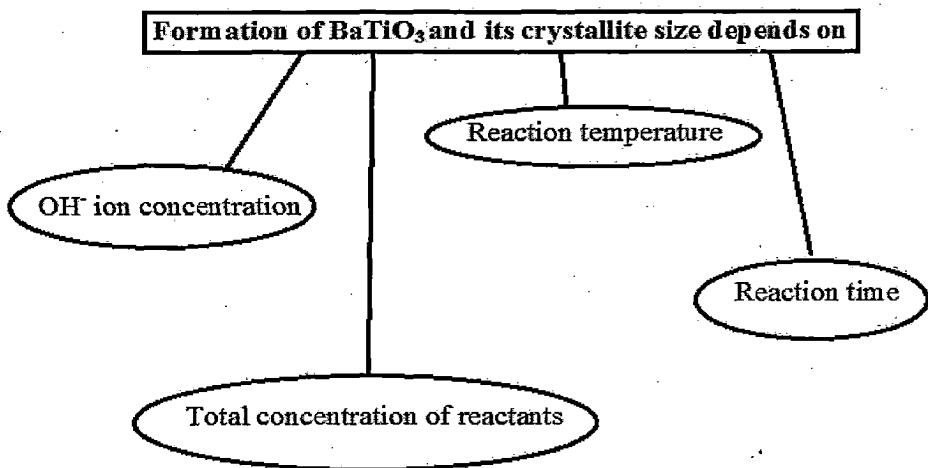
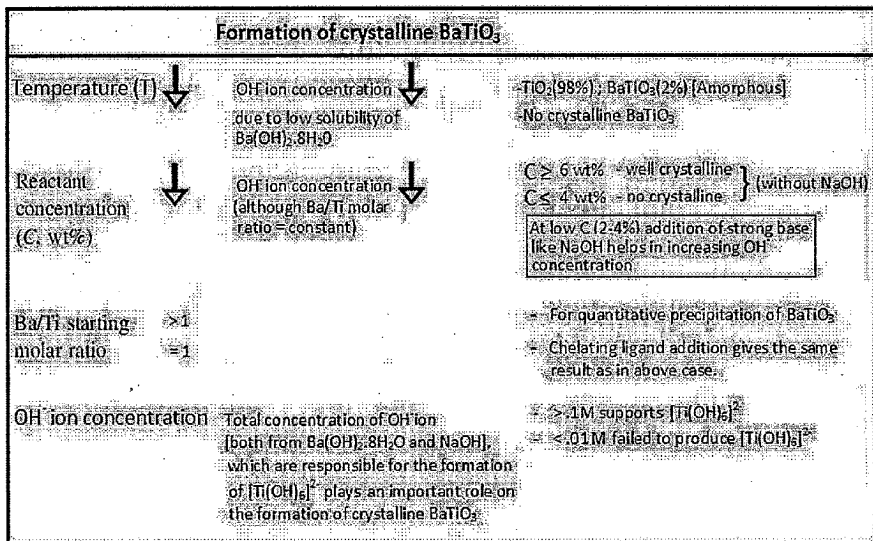
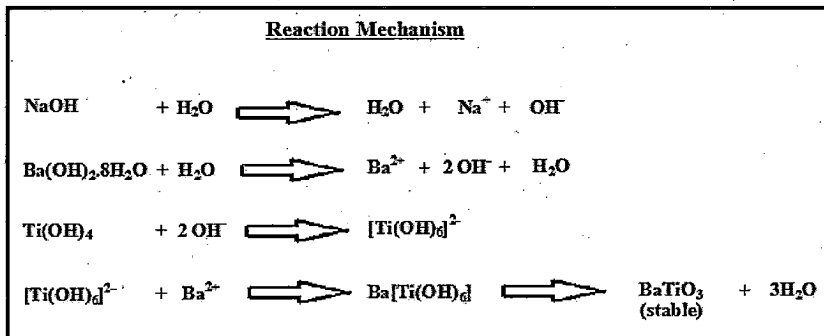


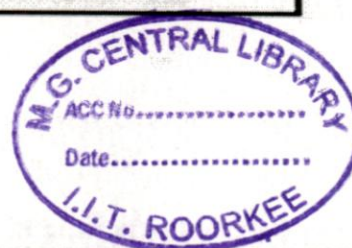
Figure 2.2 Parameters affecting the size of the crystal formed

2.2 Analysis



Variables	Crystallite Size/Reasons
T ↓	↓ Nucleation and growth process during the formation of nanocrystal. At high T, no. Of nuclei increases but the growth of crystal decreases.
C, wt% ↑	↑ Interaction among the tiny crystals are increased with the concentration
Ba/Ti } ↑ OH ⁻ ion conc } ↑	↓ Interaction among the tiny crystals Ti(OC ₂ H ₅) ₄ hydrolysed very rapidly to large number of [Ti(OH) ₆] ²⁻ nuclei, hence decreases the size
Reaction Time (t) ↑	↑ Due to growth of nanocrystals at the expense of smaller crystals with time (Ostwald ripening)

Remarks
↓ Decreases ↑ Increases — Concentration

$$C(\text{wt}\%) = \left[\frac{\text{wt. of Ba(OH)}_2 \cdot 8\text{H}_2\text{O} + \text{wt. of Ti(OC}_2\text{H}_5)_4}{\text{total wt. of the reaction mixture including solvents}} \right] \times 100$$


2.3 Characterization

Dried samples were characterized by using powder X-ray diffraction using a Scintag Pad V diffractometer system with a Cu KR beam ($\lambda = 0.1541$ nm). Morphological observation and electron diffractions (ED) on particles were confirmed on a Philips CM 200UT transmission electron microscope (TEM) with a spherical aberration coefficient (Cs) of 0.5 mm and a point-to-point resolution of 0.19 nm. The TEM was operated at an accelerating voltage of 200 kV. Scanning electron microscopy (SEM) was also conducted with a Hitachi S-3400N variable pressure microscope with a tungsten filament that delivers at least 50 nA of beam current.

2.4 Water splitting process

The experiment of water splitting to hydrogen and oxygen was carried out using a sealed glass tube and samples in water under a standard condition. Glass tubes, 0.5 in. in diameter and 1 ft in length, were used for the experiment. The reaction cell (glass tube) was filled with

nitrogen gas after adding the samples. Then ultrasonic wave vibrations using a Branson 5510-MTultrasonic cleaner were applied to 5.0mL of DI water which results in production of hydrogen gas due to the piezoelectrochemical effect between the BaTiO₃ dendrites and water.

The piezoelectricity of the material arises from the lack of inversion symmetry in their crystal structures [4]. Any deformation or strain acting on the material will cause a nonzero dipole moment in the crystal lattice. Consequently, a strain-induced charge potential is produced on the surface of the material. Specific morphological aspects of BaTiO₃ dendrites [5] will acquire electric potentials on their surfaces if an external mechanical energy is applied that results in a bending (deformation) of the dendrites. The strain induced electric potential formed on the dendritic surface in wet conditions (i.e., in pure water) is available for the reduction and oxidation reaction via charge transfer to species such as water molecules adsorbed on the surface (Figure 2.3). Note that the developed potential must be greater than the standard redox potential of water (1.23 eV) to make electrons available to initiate the redox reaction in this experiment. Residual charges or potentials lower than 1.23 eV will not participate in reactions to form H₂ and O₂ from water.

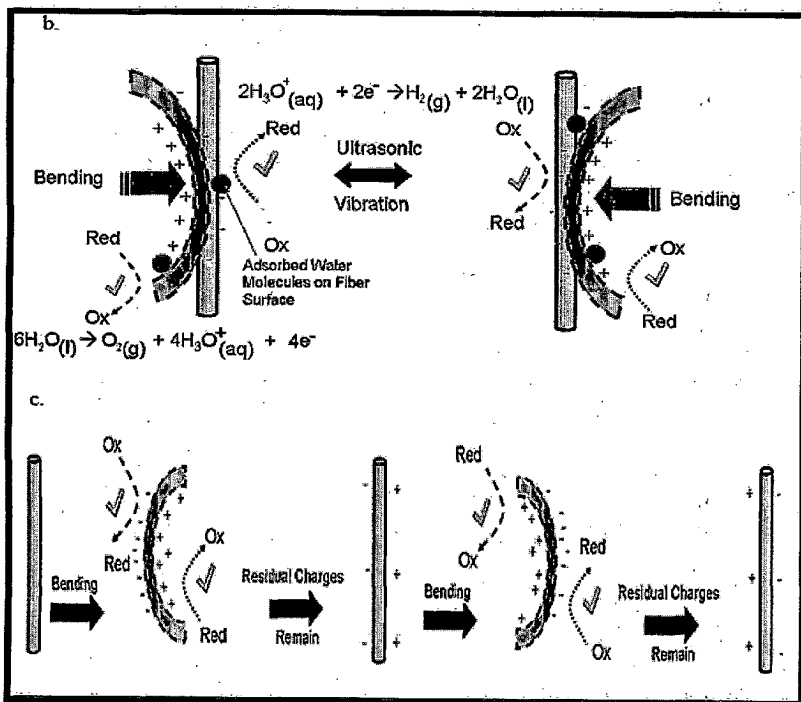
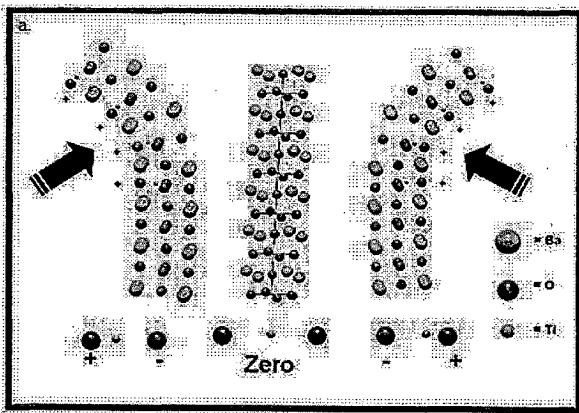


Figure 2.3 (a, b, c) Diagram shows the physics and chemistry of the reaction

To monitor the hydrogen concentration variation, the gas inside of the cell was extracted by syringe and injected into an external hydrogen analyser [6]. The amount of hydrogen gas (H_2) produced from the water splitting experiment was monitored using an AMETEC Trace Analytical ta3000 gas chromatograph equipped with a reduction gas detector (RGD) sensor for hydrogen detection. Nitrogen gas (N_2) of 99.998% purity at a flow rate of 20cc/min was applied as the carrier gas. The detection limit of the H_2 analyzer was 10 ppb hydrogen.

The hydrogen production is measured as a function of ppm vs time

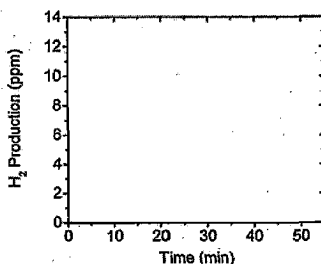


Figure 2.4 Hydrogen production vs. Time duration

2.5 PZEC efficiency Calculation

The efficiency of PZEC effect [7] is measured as a function of fiber aspect ratio. In this case, samples with different average fiber lengths were prepared by varying the synthetic time and precursor concentration during the hydrothermal process. Each sample was immersed into DI water along with ultrasonic wave vibration during the reaction. The hydrogen production performance was monitored. The efficiency of each sample was then calculated by the ratio of produced chemical potential output over the effective mechanical energy input. The value of the output chemical energy was calculated from the observed hydrogen production rate, in which the standard reduction potential of water, 1.23eV was used. In addition, in order to eliminate other factors such as surface area or secondary branches, we assume each fibre as a 3D tetragonal prism-shaped fibre with uniform width and height on the two ends, and therefore the aspect ratio is only varied by the fibre length.

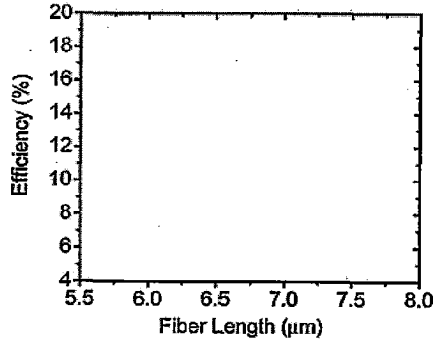


Figure 2.5 PZEC efficiency vs. fiber length

The efficiency of converting the mechanical energy from the ultrasonic waves to chemical potential driving the water splitting by piezoelectrochemical effect can be calculated as the follows.

The average output chemical potential

$$E_{chem} = \frac{2n_{H_2} E_r N_A e}{N_{fiber}} \quad (1)$$

where

n_{H_2} = hydrogen produced in moles;

E_r = threshold energy of water decomposition = 1.23 eV;

N_A = Avogadro's number;

e = electron volt,

N_{fiber} = number of fibers.

The input elastic deformation energy generated by ultrasonic wave can be found from the bending of the fibers by assuming that all the acoustic pressure is transformed into the force for fiber deformation. Accordingly, the acoustic pressure is:

$$P_A = \sqrt{2I\rho c} \quad \text{and} \quad P_{\text{effective}} = \frac{P_A}{\sqrt{2}} \quad (2)$$

where

I = acoustic intensity = 0.63 Wcm^{-2} ;

ρ = density of water;

c = speed of light in water

In addition, we assume the ultrasonic waves propagated across the system normal to the cross-section area of the reaction cell. As a result, the input mechanical energy created by ultrasonic wave vibrations acting on the fibres is

$$E_{\text{mech}} = \frac{175F^2 L^3}{4608YI} \quad (3)$$

where

F = average force acting on one fiber;

L = fiber length;

Y = Young's modulus

and I is the inertia of the fiber.

Assuming the energy did not lost in any other form, therefore, the efficiency of converting mechanical energy to chemical energy is:

$$\text{Efficiency} = \frac{E_{\text{chem}}}{E_{\text{mech}}} * 100\% \quad (4)$$

Mechanical Energy:

Acoustic Intensity from the ultrasonic generator, I_0 :

$$I_0 = \frac{\text{Watt}}{\text{cm}^2} = \frac{185(\text{W})}{24.5 * 12(\text{cm}^2)} = 0.629 \quad (5)$$

185 W = reported value from the manufacture.

24.5 x 12 = cross section area of the ultrasonic tank, in which we assume the ultrasonic wave propagates across the tank.

Reflectivity, R (reflectivity of the glass tube against the ultrasonic vibrations):

$$R = \left(\frac{\rho_{\text{glass}} c_{\text{glass}} - \rho_{\text{water}} c_{\text{water}}}{\rho_{\text{glass}} c_{\text{glass}} + \rho_{\text{water}} c_{\text{water}}} \right)^2 \quad (6)$$

$$= \left(\frac{2.8(\text{g/cm}^3) * 2\text{E}8(\text{m/s}) - 1.0(\text{g/cm}^3) * 2.25\text{E}8(\text{m/s})}{2.8(\text{g/cm}^3) * 2\text{E}8(\text{m/s}) + 1.0(\text{g/cm}^3) * 2.25\text{E}8(\text{m/s})} \right)^2$$

$$= 0.185$$

ρ = density of media

c = speed of light in media

$$I_1 = (1 - R) * I_0 = (1 - 0.185) * 0.629 = 0.513 \quad (7)$$

I_1 = transmitted acoustic intensity after the glass tube reflectivity

Therefore, the acoustic pressure:

$$P_{\text{effective}} = \frac{\sqrt{2I_1 \rho_{\text{water}} c_{\text{water}}}}{\sqrt{2}} = \sqrt{0.513 * 1.0 * 2.28\text{E}8} = 1.07\text{E}4(\text{N/m}^2) = \frac{F}{A} \quad (8)$$

A = cross section of 5 mL water in the test tube = 2.98 cm²

Next, the cross-section area of the fibre (cm²):

$$A_{fiber} = b * L \quad (9)$$

Therefore, the fraction of force acting on a fibre can be estimate:

$$F_{fiber} = \frac{F * A_{fiber}}{A} \quad (10)$$

The Young's Modulus of fibre (3) is:

$$Y = \frac{K_n L^3}{192I} \quad (14)$$

L = Fibre length

K_n = spring constant

I = fibre inertia

Finally, the mechanical energy acting on fiber causing the deformation:

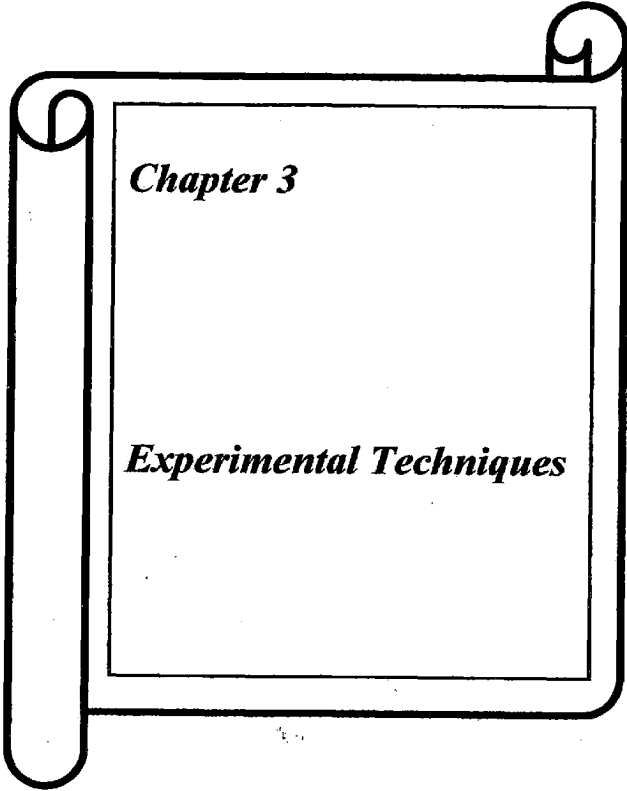
$$E_{mech} = \frac{175F_{fiber}^2 L^3}{4608YI} \quad (12)$$

Overall Efficiency:

$$Efficiency = \frac{E_{chem}}{E_{mech}} * 100\% \quad (13)$$

References

- [1] Uchino, K. Piezoelectric Actuators and Ultrasonic Motors; Kluwer Academic Publishers: London, 1997.
- [2] Herbert, J. M. Ferroelectric Transducers and Sensors; Gordon and Breach: London, 1982.
- [3] Oren, E. E.; Tas, A. C. Hydrothermal Synthesis of Dye-Doped BaTiO₃ Powders. *Metall. Mater. Trans. B* 1999, 30, 1089–1093.
- [4] Look, D. C. Recent Advances in ZnO Materials and Devices. *Mater. Sci. Eng., B* 2001, 80, 383–387.
- [5] Cao, H.; Xu, J. Y.; Zhang, D. Z.; Chang, S. H.; T., H. S.; Seeling, E. W.; Liu, X.; Chang, R. P. H. Spatial Confinement of Laser Light in Active Random Media. *Phys. Rev. Lett.* 2000, 84, 5584–5587.
- [6] Wang, Z. L. Piezoelectric Nanogenerators Based on Zinc Oxide Nanowire Arrays. *Science* 2006, 312, 242–246.
- [7] Wang, X. D.; Zhou, J. J.; Song, H.; Liu, J.; Xu, N. S.; Wang, Z. L. Piezoelectric Field Effect Transistor and Nanoforce Sensor Based on a Single ZnO Nanowire. *Nano Lett.* 2006, 6, 2768–2772.



Chapter 3

Experimental Techniques

3.1 Basic structural characterization techniques

Structural characterization of the samples has been done by using X-ray diffraction (XRD), Field emission-Scanning electron microscope (FE-SEM), Energy dispersive analysis of x-ray spectroscopy (EDAX) and Atomic force microscope (AFM). A brief description of these techniques has been made in this particular chapter.

3.1.1 X-ray diffraction (XRD)

X-ray diffraction is the non-destructive and most powerful technique for determining the crystal structure, preferred orientation, crystallite size, lattice constants, crystal defects, stress, layer thickness, phase analysis, etc. of solid matter. When a monochromatic beam of x-rays is incident upon a regular crystalline material then the beam will be scattered from the material at definite angles. This is produced by an interference effect called diffraction between the x-rays from different atomic layers within the crystal. These atomic layers are separated by distance in the order of angstroms and are comparable to the wavelength of x-rays. If the x-rays of a known frequency interacts with a crystalline solid then under particular circumstances of layer separation and angle of incidence to layer, the scattering from the different layers will constructively interfere at some angles and destructively interfere at most of the angles. This effect is characterized by the Bragg's equation ($2d \sin \theta = n\lambda$. λ = wavelength of incident radiation and d = interplanar distance between the lattice planes), which is the base of x-ray crystallography.

In the present study, Bruker D8 Advance x-ray diffractometer (Figure 2.3) was used to study the crystallinity, crystallite size and strain of the grown thin films. The radiation ($\text{Cu K}\alpha$) emanating from the X-ray tube is diffracted at the specimen and recorded by a detector. Bruker D8 Advance diffractometer uses NaI scintillation counter as a detector. It can detect

the diffracted radiations in the wavelength ranging from 0.5 to 3 Å. Monochromators are used to suppress the undesired portions of radiation. To restrict the irradiated specimen area, aperture diaphragm is arranged between the tube and the specimen as shown in **figure 2.3**. The second aperture diaphragm shields the strong scattered radiation of the first aperture diaphragm. The scattered radiation diaphragm is used to suppress undesired scattered radiation. The resolution depends upon the detector diaphragm.

The crystallographic information is obtained by evaluating d values and indexing of reflections. The characteristics diffraction pattern of a given substance can always be obtained whether the substance is present in pure state or as one constituent in a mixture of several substances. X-ray diffraction pattern is characterized by a set of line positions (2θ) and a set of relative intensities (I). The angular position of lines depends on the wavelength of the incident ray and spacing (d) of the lattice planes.

The technique can be used for quantitative analysis in which the concentration of phases are calculated by determining the area of the peak, since the intensity of diffraction lines due to one constituent of a sample depend upon the concentration of that constituent in the sample specimen. The qualitative analysis for a particular substance is accomplished by identification of the pattern of that substance. The crystallite size is an important parameter, which can be determined using Scherrer's formula (6):

$$l = \frac{0.9\lambda}{B \cos \theta_b} \quad (2.1)$$

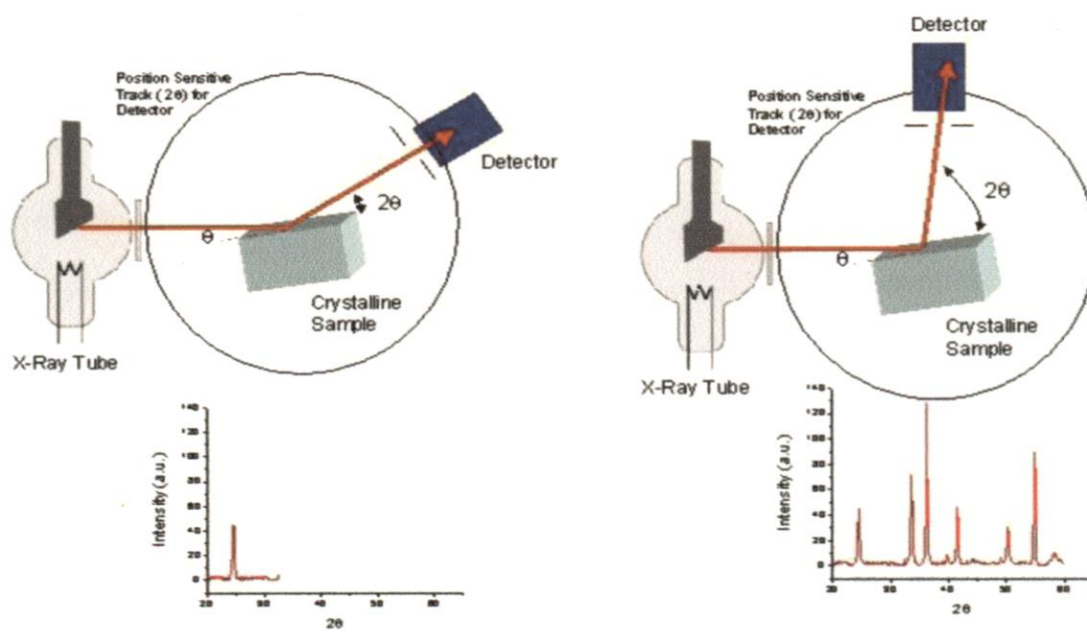


Figure 3.1 Schematic diagram of beam path.

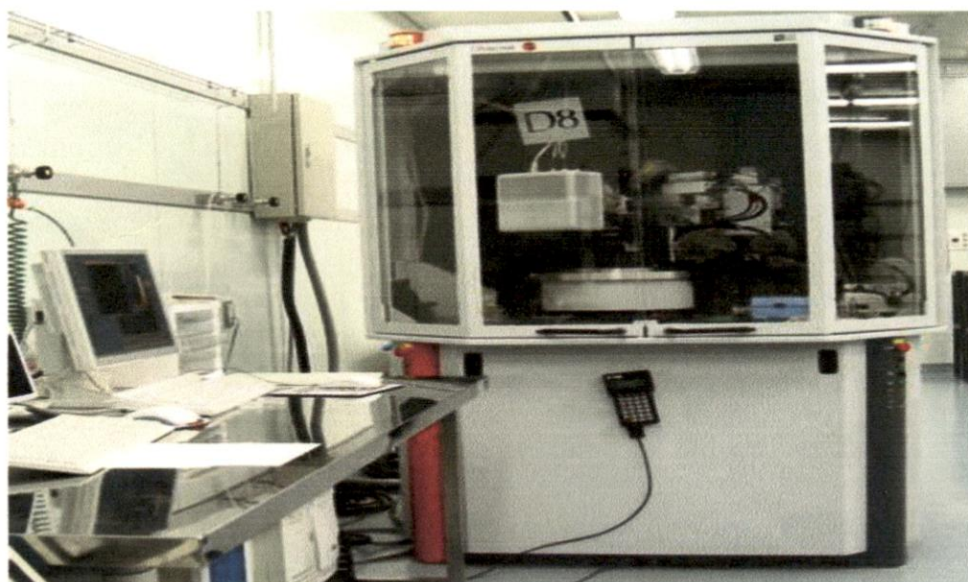


Figure 3.2 Photograph of Bruker D8 Advance X-ray Diffractometer

where l is the length of the crystal in the direction perpendicular to the reflecting planes, B is the full width at half maximum (FWHM) of the Bragg reflection in the radians on the 2θ scale and θ_b is the Bragg reflection angle. To make sure of absolute values of the 2θ diffraction angles, the diffractometer was calibrated with respect to the peak position of an Si calibration standard. A polycrystalline powder was used for instrumental correction. It is important to subtract the background and instrumental line width from the observed line width to get a correct estimate of broadening due to small particle size.

Specimen beam interaction

When an incident electron beam strikes the specimen composed of a crystalline and amorphous structure, it undergoes a series of complex interactions with the nuclei and electrons of the atoms of the sample. The interactions produce a variety of secondary products, such as:

Secondary electrons: When the specimen is struck by the primary beam, electrons are freed from the specimen. The electrons released from the surface are mostly low energy secondary electrons between 0 and 50 electron volts. They will mainly give information of morphology and topology of the specimen.

Backscattered electrons: When the specimen is struck by the primary beam, electrons are elastically and non-elastically scattered back. Elastically means the primary electrons did not lose any of their primary energy. Back-scattered electrons release information on the composition of a material, the so-called Z contrast or atomic number contrast.

Photons: Photons or light quanta are freed when the primary beam strikes a material like some minerals. These light quanta can be detected using a cathode luminescence detector. The light detected can vary from infrared to ultraviolet.

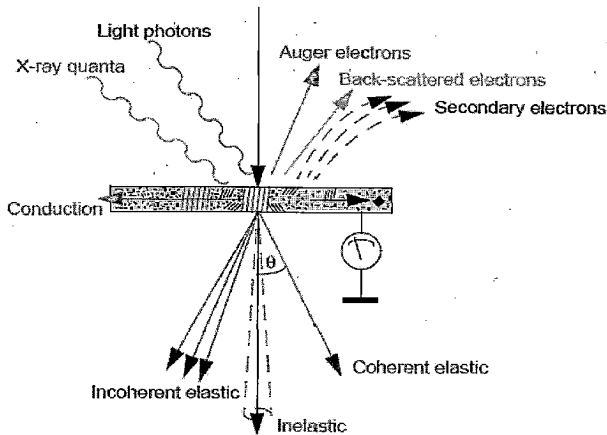


Figure 3.3 Specimen beam interaction.

Auger electrons: Due to collisions with the primary beam, auger electrons are freed. These electrons are element specific and their energy can be detected using an auger mass spectrometer. This technique is applied for detection of light elements and gives information on the top atomic layers of the specimen.

X-ray quanta: X-ray radiation takes place when an electron has received extra energy, e.g. due to a collision with an electron of the primary beam. As this is an unstable situation, the electron will fall back into its original orbit; the extra energy is released in the form of an X-ray quantum.

Conduction: Electrons that are stopped in the specimen must leave the specimen, therefore all specimens that are not conductive are made conductive by an extra layer of gold or carbon. If the specimen was non-conductive it would start to become charged and thus an unwanted electrostatic lens would be made which also increases

the inherent astigmatism.

Heat: The energy of the electrons stopped in the specimen is transferred to kinetic energy. The local temperature of the specimen can rise to temperatures higher than 100 °C. The temperature depends on the acceleration voltage, the number of electrons (emission) and size (spot size) of the primary beam. If the temperature is too high for the type of specimen under investigation, the specimen will be damaged either in the form of contamination, evaporation, or complete tearing of the film layer.

Elastic scattering: Elastic scattering takes place when the negative charged electrons are scattered due to interaction with the positively charged atomic nucleus. Because the mass of the nucleus is much higher than the mass of the electrons, therefore a negligible energy transfer takes place. This means that the speed and thus the associated wavelength of the electron do not change. There are two types of elastic scattering:

- **Incoherent elastic scattering:** This is the case when the specimen has an amorphous structure. The deflected electron waves have no phase relation to the specimen.
- **Coherent elastic scattering:** This is the case when the specimen has a crystalline structure. There is now a phase relation between the specimen and rays are deflected under defined angles.

Inelastic scattering: Inelastic scattering takes place when the negative charged electrons are scattered due to interaction with the negative charged electrons. Now energy transfer takes place, this means that the velocity and thus the associated wavelength of the electron changes.

3.1.2 Field emission scanning electron microscopy (FE-SEM)

The scanning electron microscope (SEM) has a large depth of field, which allows a large amount of the sample to be in focus at one time. The SEM also produces images of high

resolution, which means that closely spaced features can be examined at a high magnification.

In the present study, field emission scanning electron microscope (FEI Quanta 200F model) with resolution of 2 nm and magnification 500000 diameters was used to study the surface morphology of these thin films. **Figure 2.5** shows a schematic diagram of the field emission scanning electron microscope (FESEM). FESEM uses field emission electron gun, which provides improved resolution of 2 nm i.e. 3 to 6 times better than conventional SEM and minimized sample charging and damage. In conventional SEM, electrons are thermionically emitted from

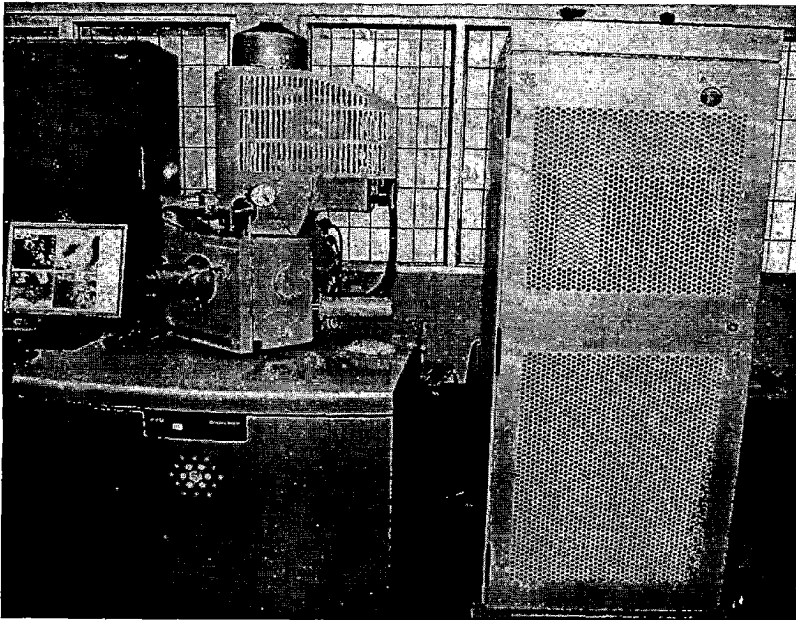


Figure 3.4 Quanta 200F FEI model of Field emission scanning electron microscope

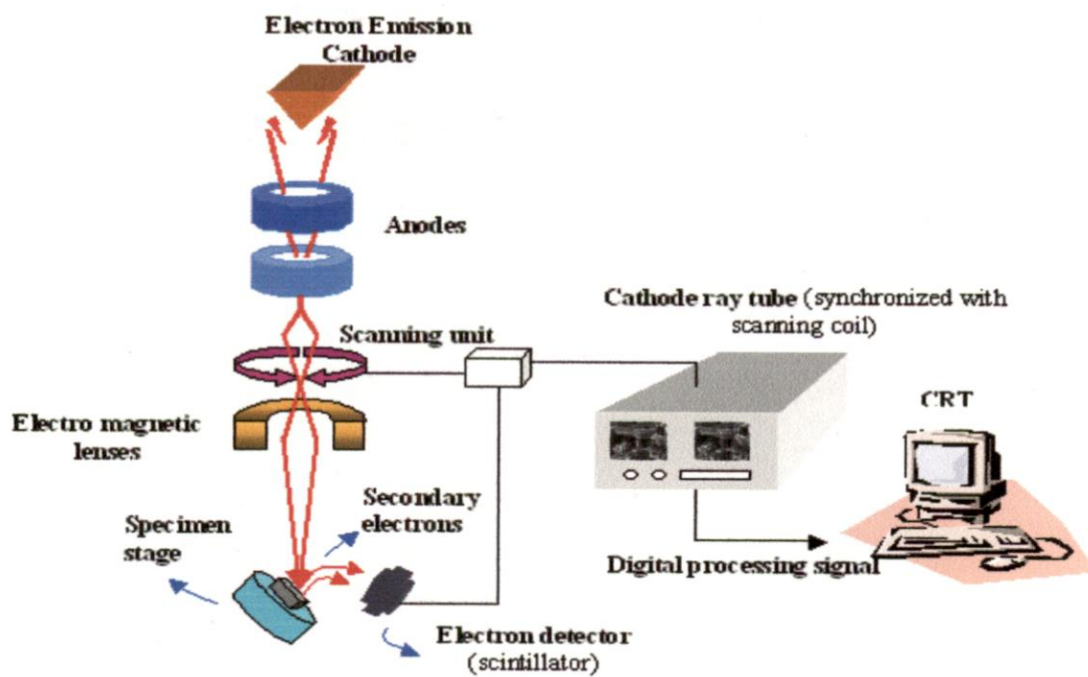
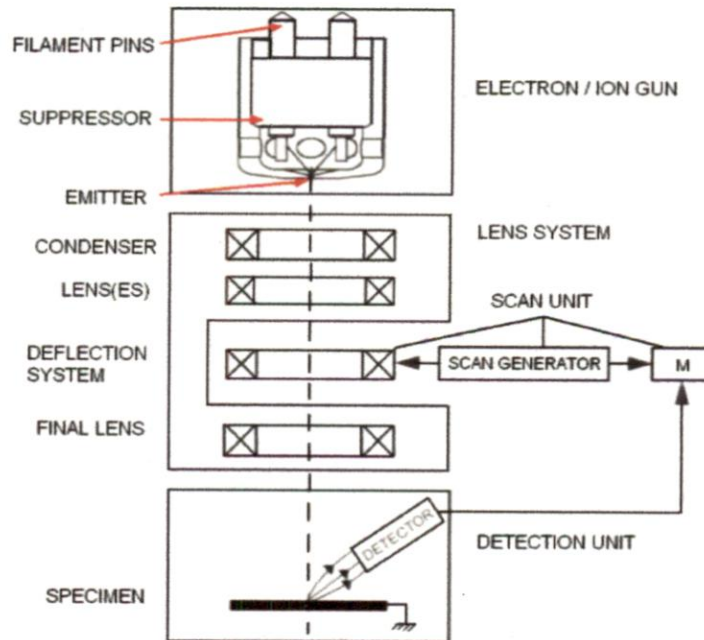


Figure 3.5 Schematic diagram of FESEM

a tungsten or lanthanum hexaboride (LaB_6) cathode and are accelerated towards an anode; alternatively electrons can be emitted via field emission (FE). Tungsten is used as a filament because it has the highest melting point and lower work function, thereby allowing it to be heated for electron emission. The basic mechanism of field emission is that a high voltage applied between a pointed cathode and a plate anode caused a current to flow. The field emission tip is generally made of a single crystal tungsten wire sharpened by electrolytic etching. A tip diameter of 100 to 1000 Å is used. The field emission process itself depends on the work function of the metal, which can be affected by adsorbed gases.

The electron beam, which typically has an energy ranging from a few hundred eV to 50 keV, is focused by two condenser lenses into a beam with a very fine focal spot size. The first condenser lens that works in conjunction with the condenser aperture helps to narrow the beam and also limit its current. The second condenser lens then forms the electrons into a very thin, coherent beam. The high-energy beam of electrons scans the sample surface in a raster pattern using a set of scanning coils to obtain image. The objective lens does the final focusing of the beam onto the sample. At each point the numbers of secondary and back-scattered electrons reaching the detector are counted to be used for determining the relative intensity of the pixel representing that point in the final image.

Using the energy dispersive x-ray analysis (EDAX) attachment with the FE-SEM, elemental composition analysis was done. An EDAX spectrum normally displays peaks corresponding to the energy levels for which the most X-rays had been received. Each of these peaks is unique to an atom, and therefore corresponds to a single element. Higher the peak intensity, higher is the element concentration in the specimen.

Insulator samples would be difficult to image using an SEM because of the fact that they would develop a negative charge (due to build-up of electrons), which would cause the image to become defocused due to deflection of the exciting electron beam, abnormal contrast in the image due to the uneven distribution of the negative charge on the sample and breaks or splitting of the image due to high negative charge on the sample which deflects the beam of electrons. Therefore, in order to enhance the number of secondary electrons from an insulating sample, the sample is often coated with a thin layer of gold-palladium or another electron-rich conducting material that produces abundant secondary electrons when struck by a focused electron beam. A thin metal coating will not mask surface features or the overall topology of the underlying sample. The conducting coating also conducts electrons away, so that the sample does not develop a significant charge when it loses secondary electrons and other types of electrons. This type of coating is essential for insulator samples, which do not conduct charged particles.

Energy Dispersive X-ray Spectroscopy (EDXS)

Energy dispersive X-ray spectroscopy is an analytical tool predominantly used for chemical characterization. Being a type of spectroscopy, it relies on the investigation of a sample through interactions between light and matter, analyzing X-rays in its particular case. The emitted characteristic X-rays may be analyzed for their energy and intensity, the energy being the signature of the element emitting them and the intensity as to how much of it is present. Detection of X-ray by energy dispersive spectrometer is accomplished by employing a detector which is a negatively biased Si chip into which lithium has been diffused and onto which a thin contact Au layer has been evaporated.

3.2 Hydrothermal synthesis

Hydrothermal synthesis [1] includes the various techniques of crystallizing substances from high-temperature aqueous solutions at high vapor pressures; also termed "hydrothermal method". Hydrothermal synthesis can be defined as a method of synthesis of single crystals that depends on the solubility of minerals in hot water under high pressure. The crystal growth is performed in an apparatus consisting of a steel pressure vessel called autoclave, in which a nutrient is supplied along with water. One type of solution growth from water at high temperatures and pressure is known as the hydrothermal technique.

In the hydrothermal process (flux technique) [2] crystals are grown directly from the molten solvent. This process utilizes powdered chemicals of the correct composition and adds a liquid solution to dissolve the compound before super heating. The dissolved solution is known as a flux. As the solvent evaporates and the flux begins to slowly cool and crystallize.

Hydrothermal synthesis is a method that is widely used for the production of (ultra) small powders and particles especially in the ceramics industry. Recent research has showed the possibility of using this method for the synthesis of nanometer-sized objects as carbon nanotubes or nanowires.

Hydrothermal techniques are a particular case of solvothermal processes that operate basically on the principle of small crystals growing from solutions at high pressures and high temperatures. The method produces submicrometer and nanometer sized nanopowders without additional physical and chemical reaction steps.

3.2.1 Volumetric flask

A volumetric flask (figure 3.6 d) is a piece of laboratory glassware, a type of laboratory flask, used in analytical chemistry for the preparation of solutions. It is made of glass or plastic and consists of a flat bottomed bulb with a long neck, usually fitted with a stopper. The stopper is normally made in a chemically resistant plastic such as polypropylene rather than glass. The neck has a single ring graduation mark and a label. The label should show the nominal volume, tolerance, calibration temperature, class, relevant manufacturing standard. Volumetric flasks are used for making up solutions to a known volume.

3.2.2 Teflon (PTFE) container

PTFE is most well-known by the Teflon. PTFE is a fluorocarbon solid, as it is a high-molecular-weight compound consisting wholly of carbon and fluorine. PTFE is hydrophobic: neither water nor water-containing substances wet PTFE, as fluorocarbons demonstrate mitigated London dispersion forces due to the high electronegativity of fluorine. PTFE has one of the lowest coefficients of friction against any solid.

It is very non-reactive, partly because of the strength of carbon-fluorine bonds, and so it is often used in containers and pipework for reactive and corrosive chemicals.

Combined with its high melting temperature, this makes it the material of choice as a high-performance substitute for the weaker and lower melting point polyethylene. Because of its chemical inertness, PTFE cannot be cross-linked like an elastomer. Therefore, it has no "memory" and is subject to creep. This is advantageous when used as a seal, because the material creeps a small amount to conform to the mating surface.

3.2.3 Stainless Steel Autoclave

An autoclave (figure 3.6 b) is an oven-like device with features similar to a pressure cooker that allows the heating of aqueous solutions to higher temperatures than water's boiling point in order to sterilize the contents of the autoclave. A strong sealed vessel used for chemical reactions at high pressure. Stainless Steel Containers are a smart choice for solids, liquids and intermediate products. Stainless steel provides superior corrosion resistance.

3.2.4 Electric Furnace

Electric furnace (figure 3.6 e) is used for heating purpose in various industrial production processes. Electric furnaces are used where more accurate temperature control is required. In resistance heating furnaces, the resistance heating elements are used to generate the heat in a heating chamber. The heating elements used are Nichrome wire, Kanthal wire or Graphite rods depending upon the temperature requirements. The unit proposed in this project profile envisages manufacturing furnaces to a maximum temperature of 1000⁰C and only up to 50 kW power rating. In this case, Kanthal wire is used. The temperature is controlled using thermostats and the temperature is monitored by thermocouples. The heating chamber is constructed by M. S. Sheets and channels and for thermal insulation, fire clay bricks and refractory bricks are used.

A Furnace essentially consists of a chamber in which the materials to be heated are placed. Heat is supplied to this chamber from the resistance heating elements placed around the chamber. Heat is transmitted to the object by radiation. M.S. Sheets and channels construct the chamber. Then the chamber is lined with fire clay bricks. Fire clay bricks provide thermal insulation. After this a lining with refractory bricks is made. Heating elements are embedded

on the refractory lining. Suitable groves will be provided to accommodate the heating elements on the refractory lining. The terminals of the heating elements are taken out for connecting to the electric power supply.

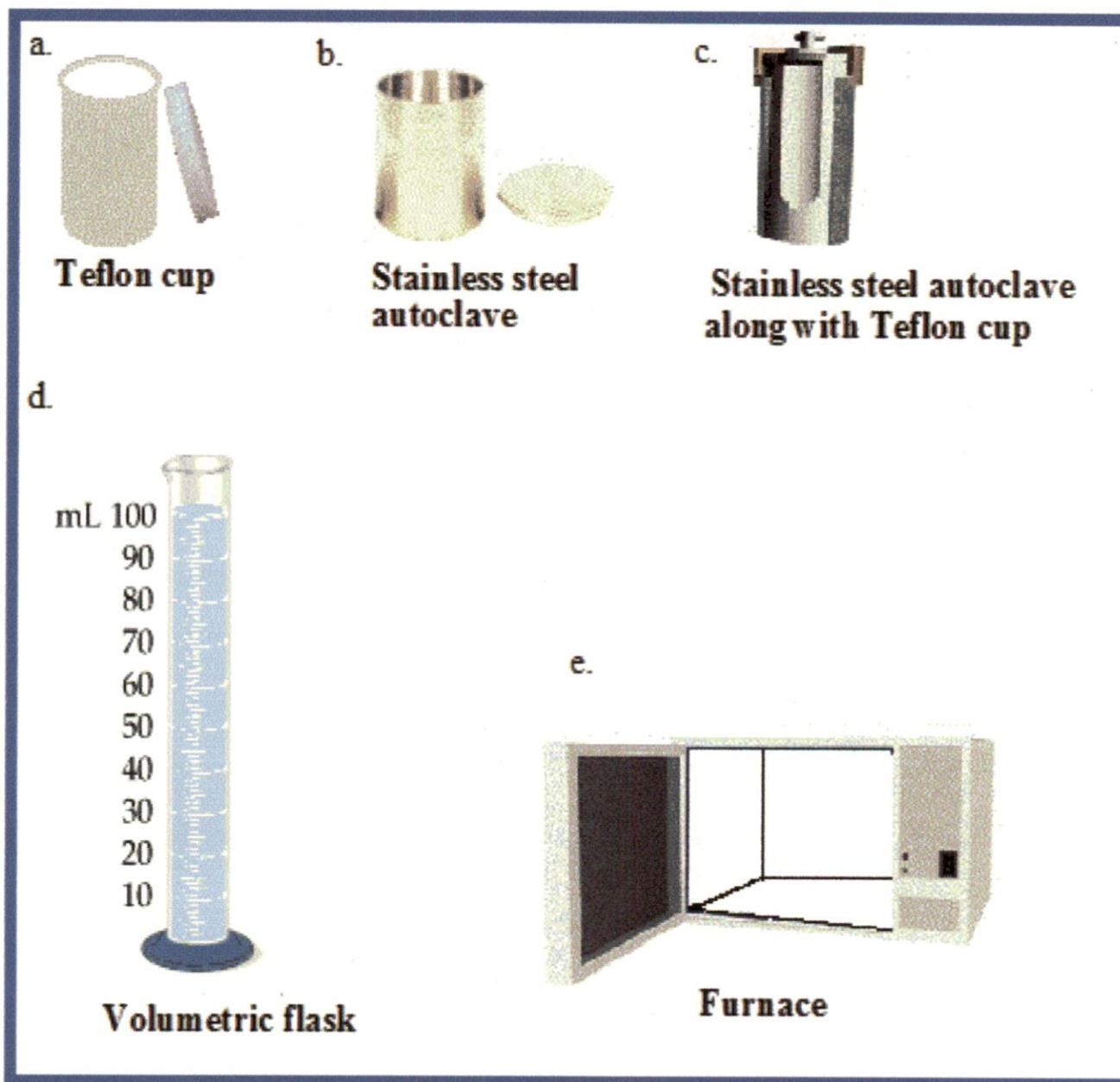


Figure 3.6 Equipments used for hydrothermal synthesis process

3.3 Water splitting process

Water splitting is the general term for a chemical reaction in which water is separated into oxygen and hydrogen. There are several methods for this process but in this thesis work the method used is based on piezoelectric property of the piezoelectric materials.

Materials that can produce electricity are at the core of piezoelectric research and the vision of self-powering machines and devices. With the use of nanomaterials, the field of has experienced a lot of new and interesting research efforts. When pulsed with ultrasonic vibrations, the nanofibers flexed and catalyzed a chemical reaction to split the water molecules into hydrogen and oxygen. When the fibers bend, asymmetries in their crystal structures generate positive and negative charges and create an electrical potential. This phenomenon, called the piezoelectric effect, has been well known in certain crystals. However, while the bulk materials are brittle, at the nanoscale they are flexible.

Under the impact of the ultrasonic vibrations, the nanofibers flexed and catalyzed a chemical reaction to split the water molecules into hydrogen and oxygen. The physics and chemistry of generating hydrogen and oxygen gases from pure water arise from the combination of piezoelectric properties of the nanofibers and the redox reaction of water. The piezoelectricity of each material arises from the lack of inversion symmetry in their crystal structures. Any deformation or strain acting on the material will cause a nonzero dipole moment in the crystal lattice. Consequently, a strain-induced charge potential is produced on the surface of the material. The strain-induced electric potential formed on the surface of the nanofiber in wet conditions (i.e., in pure water) is then available for the reduction and oxidation reaction via charge transfer to water molecules adsorbed on the surface. However the developed potential must be greater than the standard redox potential of water (1.23 eV) to make electrons

available to initiate the redox reaction in such a setup. Smaller fibers, especially on the nanoscale, bend more easily than larger crystals and therefore also produce electric charges easily.

3.3.1 Vacuum Pump

A vacuum pump is a device that removes gas molecules from a sealed volume in order to leave behind a partial vacuum. Positive displacement pumps are the most effective for low vacuums. Momentum transfer pumps in conjunction with one or two positive displacement pumps are the most common configuration used to achieve high vacuums. In this configuration the positive displacement pump serves two purposes. First it obtains a rough vacuum in the vessel being evacuated before the momentum transfer pump can be used to obtain the high vacuum, as momentum transfer pumps cannot start pumping at atmospheric pressures. Second the positive displacement pump backs up the momentum transfer pump by evacuating to low vacuum the accumulation of displaced molecules in the high vacuum pump.

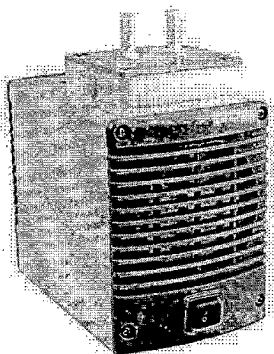


Figure 3.7 Vacuum pump

Laboratory Vacuum Pump 6 l	
Delivery	6 (l/min)
Absolute Vacuum	100 (mbar)
Operating Pressure (max)	2.5 (bar)
Connectors for Tube	ID 4 (mm)
Ambient Temperature	5 ... 40°C
Mains 16694-2-50...	230 V/50 Hz
Mains 16694-1-60...	115 V/60 Hz
Motor Protection	IP 20
Power P1	65 W
Operating Current	0.63 A
Weight	1.9 kg
Dimensions LxHxW (mm)	164x141x90

Table 3.1 Technical specifications of the vacuum pump

Characteristic set-up of a laboratory vacuum filtration

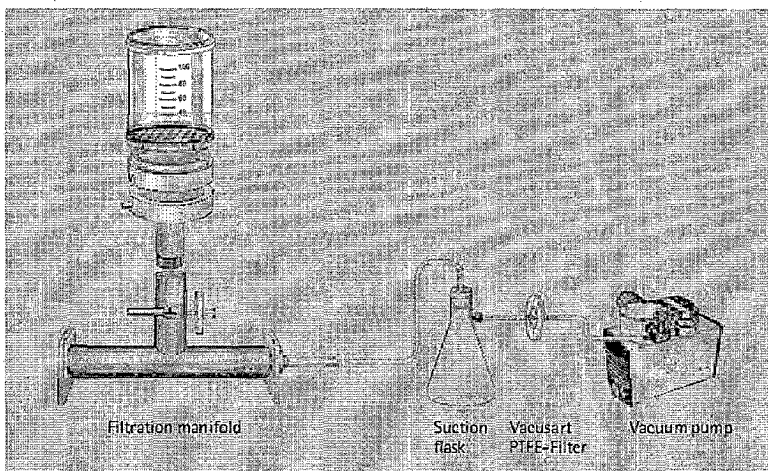


Figure 3.8 Characteristic set up of a laboratory vacuum filtration

3.3.2 Ultrasonic Cleaner

An ultrasonic cleaner [3], sometimes called a sonicator, is a cleaning device that uses ultrasound (usually from 20–400 kHz) and an appropriate cleaning solvent (sometimes ordinary tap water) to clean delicate items. The ultrasound can be used with only water but solvent is advised; it enhances the effect of a solvent. Ultrasonic cleaners are often used to clean jewellery, lenses and other optical parts but sometimes it can also be used for the purposes where the ultrasonic waves of the given frequencies are required like in experimental works.

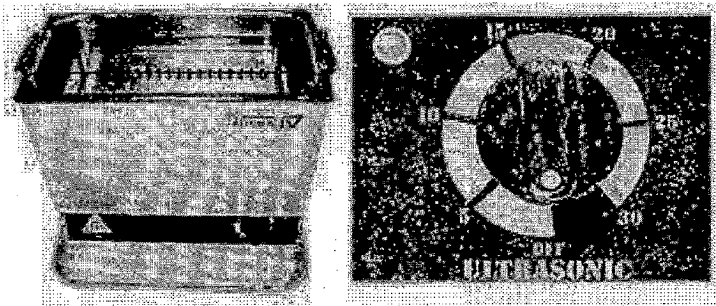


Figure 3.9 Ultrasonic cleaner

Process characteristics

Ultrasonic cleaner uses high frequency sound waves to agitate in an aqueous solution [4]. Cavitation bubbles induced by the agitation act on contaminants adhering to substrates like metals, plastics, glass, rubber, and ceramics. This action also penetrates blind holes, cracks,

and recesses. The intention is to thoroughly remove all traces of contamination tightly adhering or embedded onto solid surfaces. Water or other solvents can be used, depending on the type of contamination and the workpiece. Contaminants can include dust, dirt, oil, pigments, grease, polishing compounds, flux agents, fingerprints, soot wax and mold release agents, biological soil like blood, and so on. Ultrasonic cleaning can be used for a wide range of workpiece shapes, sizes and materials, and may not require the part to be disassembled prior to cleaning.

Design and operating principle

In an ultrasonic cleaner, the object to be cleaned is placed in a chamber containing a suitable solution (in an aqueous or organic solution, depending on the application). In aqueous cleaners, the chemical added is a surfactant which breaks down the surface tension of the water base. An ultrasound generating transducer built into the chamber, or lowered into the fluid, produces ultrasonic waves in the fluid by changing size in concert with an electrical signal oscillating at ultrasonic frequency. This creates compression waves in the liquid of the tank which 'tear' the liquid apart, leaving behind many millions of microscopic 'voids' or 'partial vacuum bubbles' (cavitation). These bubbles collapse with enormous energy; temperatures and pressures on the order of 5,000 K and 20,000 lbs per square inch are achieved however, they are so small that they do no more than clean and remove surface dirt and contaminants. The higher the frequency, the smaller the nodes between the cavitation points, which allows for cleaning of more intricate detail.

Transducers are usually made of piezoelectric material (e.g. lead zirconate titanate or barium titanate), and sometimes magnetostrictive (made of a material such as nickel or ferrite). The

often harsh chemicals used as cleaners in many industries are not needed, or used in much lower concentrations, with ultrasonic agitation. Ultrasonics are used for industrial cleaning, and also used in many medical and dental techniques and industrial processes.

3.4 Hydrogen gas detection technique

3.4.1 Gas Chromatography

Gas-liquid chromatography (GLC) or simply gas chromatography (GC) [5] is a type of chromatography in which the mobile phase is a carrier gas, usually an inert gas such as helium or an unreactive gas such as nitrogen, and the stationary phase is a microscopic layer of liquid or polymer on an inert solid support, inside glass or metal tubing, called a column. The instrument used to perform gas chromatographic separations is called a gas chromatograph. Gas Chromatography is different from other forms of chromatography (HPLC, TLC, etc.) because the solutions travel through the column in a gas state. The interactions of these gaseous analytes with the walls of the column (coated by different stationary phases) causes different compounds to elute at different times called retention time. The comparison of these retention times is the analytical power to GC. This makes it very similar to HPLC.

A gas chromatograph is a chemical analysis instrument for separating chemicals in a complex sample. A gas chromatograph uses a flow-through narrow tube known as the column through which different chemical constituents of a sample pass in a gas stream (carrier gas, mobile phase) at different rates depending on their various chemical and physical properties and their interaction with a specific column filling, called the stationary phase. As the chemicals exit the end of the column, they are detected and identified electronically. The function of the stationary phase in the column is to separate different components, causing each one to exit

the column at a different time (retention time). Other parameters that can be used to alter the order or time of retention are the carrier gas flow rate, and the temperature.

Principle:-

In a GC analysis, a known volume of gaseous or liquid analyte is injected into the column, usually using a micro syringe. As the carrier gas sweeps the analyte molecules through the column, this motion is inhibited by the adsorption of the analyte molecules either onto the column walls or onto packing materials in the column. The rate at which the molecules progress along the column depends on the strength of adsorption, which in turn depends on the type of molecule and on the stationary phase materials. Since each type of molecule has a different rate of progression, the various components of the analyte mixture are separated as they progress along the column and reach the end of the column at different times (retention time). A detector is used to monitor the outlet stream from the column; thus, the time at which each component reaches the outlet and the amount of that component can be determined. Generally, substances are identified (qualitatively) by the order in which they emerge (elute) from the column and by the retention time of the analyte in the column.

Different parts of Gas Chromatography:-**Auto samplers**

The auto sampler provides the means to introduce automatically a sample into the inlets. Manual insertion of the sample is possible but is no longer common. Automatic insertion provides better reproducibility and time-optimization. Different kinds of auto samplers exist. Auto samplers can be classified in relation to sample analysis:

- Liquid
- Static head-space by syringe technology
- Dynamic head-space by transfer-line technology

Inlets

The column inlet -provides the means to introduce a sample into a continuous flow of carrier gas. The inlet is a piece of hardware attached to the column head , a sample is introduced into a heated small chamber via a syringe through a septum the heat facilitates volatilization of the sample and sample matrix. The carrier gas then either sweeps the entirety splitless/ mode or a portion of the sample into the column.

Gas source inlet - The carrier gas flow is not interrupted while a sample can be expanded into a previously evacuated sample loop. Upon switching, the contents of the sample loop are inserted into the carrier gas stream.

Purge and Trap system- An inert gas is bubbled through an aqueous sample causing insoluble volatile chemicals to be purged from the matrix. The volatiles are 'trapped' on an absorption column (known as a trap or concentrator) at ambient temperature. The trap is then heated and the volatiles are directed into the carrier gas stream. SPME (solid phase micro extraction) offers a convenient, low-cost alternative to Purge and trap systems with the versatility of a syringe and simple use of the S/SL port.

Columns:-

Two types of columns are used in GC -

- Packed columns

They are 1.5 - 10 m in length and have an internal diameter of 2 - 4 mm. The tubing is usually made of stainless steel or glass and contains a packing of finely divided, inert solid support material that is coated with a liquid or solid stationary phase. The nature of the coating material determines what type of materials will be most strongly adsorbed.

- **Capillary columns**

They have a very small internal diameter, on the order of a few tenths of millimeters, and lengths between 25-60 meters are common. The inner column walls are coated with the active materials some columns are quasi solid filled with many parallel micro pores. Most capillary columns are made of fused-silica with a polyimide outer coating. These columns are flexible, so a very long column can be wound into a small coil.

Detectors:-

A number of detectors are used in gas chromatography. The most common are the flame ionization detector (FID) and the thermal conductivity detector (TCD). Both are sensitive to a wide range of components, and both work over a wide range of concentrations. While TCDs are essentially universal and can be used to detect any component other than the carrier gas (as long as their thermal conductivities are different than that of the carrier gas, at detector temperature), FIDs are sensitive primarily to hydrocarbons, and are more sensitive to them than TCD. However, an FID cannot detect water. Both detectors are also quite robust. Since TCD is non-destructive, it can be operated in-series before an FID (destructive), thus providing complementary detection of the same eluents.

Other detectors are sensitive only to specific types of substances, or work well only in narrower ranges of concentrations. They include:-

- Discharge ionization detector (DID)
- Electron capture detector (ECD)
- Flame photometric detector (FPD)
- Hall electrolytic conductivity detector (EICD)
- Helium ionization detector (HID)
- Nitrogen phosphorus detector (NPD)
- Mass selective detector (MSD)
- Photo-ionization detector (PID)
- Pulsed discharge ionization detector (PDD)
- Thermal energy analyzer (TEA)

Some gas chromatographs are connected to a mass spectrometer which acts as the detector. The combination is known as GC-MS. Some GC-MS are connected to an NMR spectrometer which acts as a backup detector. This combination is known as GC-MS-NMR. Some GC-MS-NMR are connected to an infrared spectrophotometer which acts as a backup detector. This combination is known as GC-MS-NMR-IR. It must, however, be stressed this is very rare as most analyses needed can be concluded via purely GC-MS [6].

Operating Variables:-

- **Carrier gas selection and flow rates**

Typical carrier gases include helium, nitrogen, argon, hydrogen and air. Which gas to use is usually determined by the detector being used? When analyzing gas samples, however, the carrier is sometimes selected based on the sample's matrix. Safety and availability can also influence carrier selection, for example, hydrogen is flammable, and high-purity helium can

be difficult to obtain in some areas. The purity of the carrier gas is also frequently determined by the detector, though the level of sensitivity needed can also play a significant role.

The higher the flow rates the faster the analysis, but the lower the separation between analytes. Selecting the flow rate is therefore the same compromise between the level of separation and length of analysis as selecting the column temperature. With GCs made before the 1990s, carrier flow rate was controlled indirectly by controlling the carrier inlet pressure, or "column head pressure." The actual flow rate was measured at the outlet of the column or the detector with an electronic flow meter, or a bubble flow meter. The pressure setting was not able to be varied during the run, and thus the flow was essentially constant during the analysis. Many modern GCs, however, electronically measure the flow rate, and electronically control the carrier gas pressure to set the flow rate.

- **Inlet types and flow rates**

The choice of inlet type and injection technique depends on if the sample is in liquid, gas, adsorbed, or solid form, and on whether a solvent matrix is present that has to be vaporized. Dissolved samples can be introduced directly onto the column via a COC injector, if the conditions are well known, if a solvent matrix has to be vaporized and partially removed, a S/SL injector is used (most common injection technique) gaseous samples (e.g. air cylinders) are usually injected using a gas switching valve system, adsorbed samples (e.g. adsorbent tubes) are introduced using either an external (on-line or off-line) desorption apparatus such as a purge-and-trap system, or are desorbed in the S/SL injector (SPME applications).

- **Sample injection technique**

The injection system, in the capillary gas chromatograph, should fulfill the following two requirements:

- The amount injected should not overload the column.
- The width of the injected plug should be small compared to the spreading due to the chromatographic process.

Some general requirements, which a good injection technique should fulfill are-

- It should be possible to obtain the column's optimum separation efficiency.
 - It should allow accurate and reproducible injections of small amounts of representative samples.
 - It should induce no change in sample composition. It should not exhibit discrimination based on differences in boiling point, polarity, concentration or thermal/catalytic stability.
- **Column temperature**

The column in a GC is contained in an oven, the temperature of which is precisely controlled electronically. The rate at which a sample passes through the column is directly proportional to the temperature of the column. The higher the column temperature, the faster the sample moves through the column. However, the faster a sample moves through the column, the less it interacts with the stationary phase, and the less the analytes are separated. In general, the column temperature is selected to compromise between the length of the analysis and the level of separation. A method which holds the column at the same temperature for the entire analysis is called "isothermal". A temperature program allows analytes that elute early in the analysis to separate adequately, while shortening the time it takes for late-eluting analytes to pass through the column.

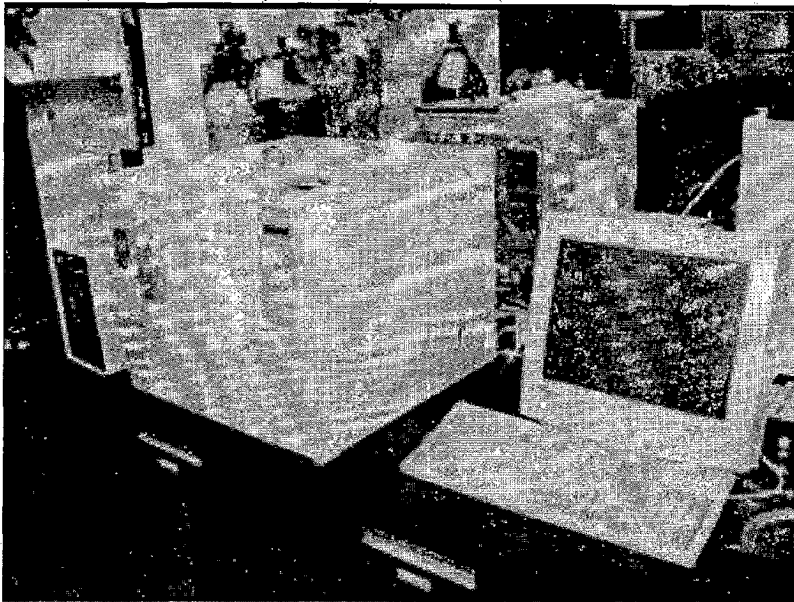


Figure 3.10 Set up of Gas chromatography

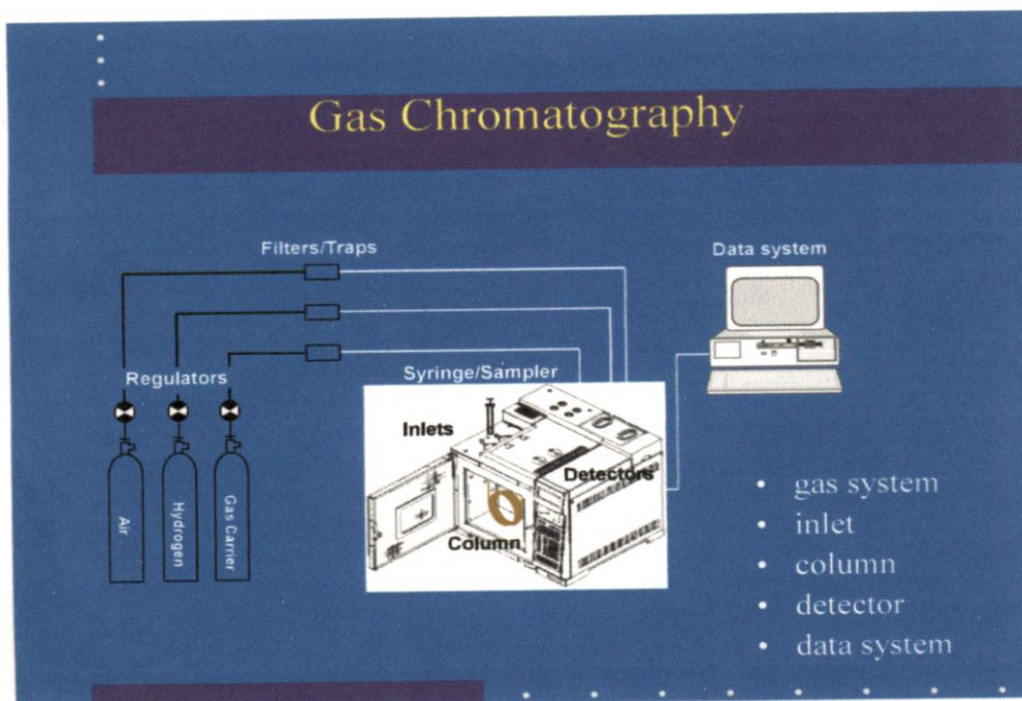


Figure 3.11 Line diagram of Gas Chromatography

Procedure:-

1. Obtain the initial oven temperature based on type of sample.
2. Take a sample in syringe and enter it into column inlet synchronize with start option in computer for analysis
3. Start the ramp input.
4. Measure the area and retention time of graph correspond to analysis sample.
5. Make a calibration chart based on different concentration with area of the peak measured.

References

- [1] Hydrothermal Crystal Growth - Quartz". Roditi International. Retrieved 2006-11-17.
- [2] Laudise, R.A. (1958). R.H. Doremus, B.W. Roberts and D. Turnbull. ed. Growth and perfection of crystals. Proceedings of an International Conference on Crystal Growth held at Cooperstown, New York on August 27–29, 1958.. Wiley, New York. pp. 458–463.
- [3] Robert H. Todd, Dell K. Allen, and Leo Alting; Manufacturing Processes Reference Guide
- [4]A. Henglein and M.J. Gutierrez., J. Phys. Chem. 97, 158, 1993
- [5] Pavia, Donald L., Gary M. Lampman, George S. Kriz, Randall G. Engel (2006). Introduction to Organic Laboratory Techniques (4th Ed.). Thomson Brooks/Cole. pp. 797–817.
- [6] Harris, Daniel C. (1999), "24. Gas Chromatography", Quantitative chemical analysis (Chapter) (Fifth ed.), W. H. Freeman and Company, pp. 675–712.



Chapter 4

***Hydrothermal Synthesis
and Characterization of
BaTiO₃ Nano crystals***

4.1 Hydrothermal synthesis

BaTiO₃ single crystal can be prepared by various methods but in this experiment we use hydrothermal process for the synthesis. In this experiment we made three samples to get three crystals of different fibre lengths, which will be further used to calculate the PZEC efficiency [3] at different fibre lengths.

Hydrothermal synthesis [1] can be defined as a method of synthesis of single crystals that depends on the solubility of minerals in hot water under high pressure. The crystal growth is performed in an apparatus consisting of a steel pressure vessel called autoclave, in which a nutrient is supplied along with water.

Although melt growth techniques provide for rapid growth and are basically simpler and easier to control than techniques starting from solution, there are certain materials where melt techniques cannot be used. In the case of quartz where the melt is too viscous, or in the case emeralds where the melt is immiscible, solution growth in one of its variants is more suitable.

One type of solution growth from water at high temperatures and pressure is known as the hydrothermal technique. In the hydrothermal process (flux technique) crystals are grown directly from the molten solvent. This process utilizes powdered chemicals of the correct composition and adds a liquid solution to dissolve the compound before super heating. The dissolved solution is known as a flux. As the solvent evaporates and the flux begins to slowly cool and crystallize.

Hydrothermal synthesis [2] is a method that is widely used for the production of (ultra) small powders and particles especially in the ceramics industry. Recent research has showed the

possibility of using this method for the synthesis of nanometer-sized objects as carbon nanotubes or nanowires.

Hydrothermal techniques are a particular case of solvothermal processes [4] that operate basically on the principle of small crystals growing from solutions at high pressures and high temperatures. The method produces submicrometer and nanometer sized nanopowders without additional physical and chemical reaction steps.

Possible advantages of the hydrothermal method over other types of crystal growth include the ability to create crystalline phases which are not stable at the melting point. Also, materials which have a high vapour pressure near their melting points can also be grown by the hydrothermal method. The method is also particularly suitable for the growth of large good-quality crystals while maintaining good control over their composition. Disadvantages of the method include the need of expensive autoclaves, and the impossibility of observing the crystal as it grows [5].

4.1.1 Equipment for hydrothermal crystal growth

The crystallization vessels used are autoclaves. These are usually thick-walled steel cylinders with a hermetic seal which must withstand high temperatures and pressures for prolonged periods of time. Furthermore, the autoclave material must be inert with respect to the solvent. The closure is the most important element of the autoclave.

To prevent corrosion of the internal cavity of the autoclave, protective inserts are generally used. These may have the same shape of the autoclave and fit in the internal cavity (contact-type insert) or be a "floating" type insert which occupies only part of the autoclave interior.

Inserts may be made of carbon-free iron, copper, silver, gold, platinum, titanium, glass (or quartz), or Teflon, depending on the temperature and solution used.

4.2 Experimental details

The experiment needs the following equipments and chemicals:

- Chemicals :
 - Titanium hydroxide - Ti(OH)₄(s)
 - Barium hydroxide octahydrate - Ba(OH)₂.8H₂O(s)
 - Sodium hydroxide - NaOH(s)
- Equipments :
 - Stainless-steel container
 - Teflon container
 - Closed bomb
 - Graduated Glass beaker
 - Volumetric flask
 - Sample(s) Weighing machine



Teflon cup



Stainless steel autoclave



Stainless steel autoclave along with Teflon cup



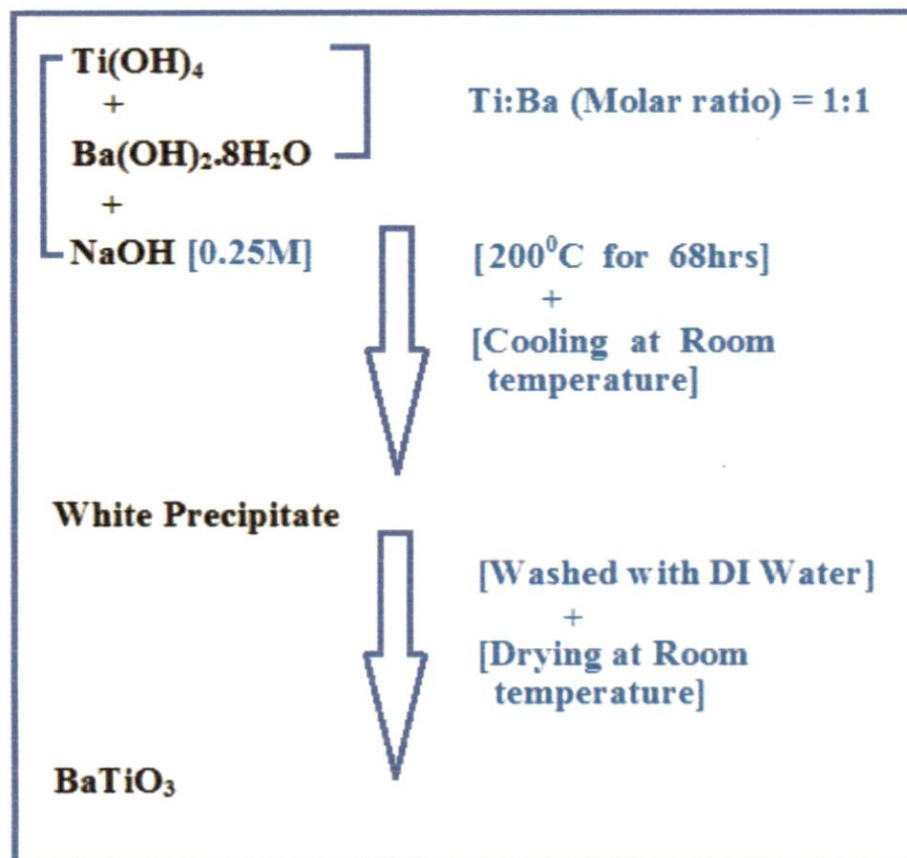
Sample(s) Weighing machine



Furnace

Figure 4.1 Equipments used for hydrothermal process

All of the chemicals that were used as starting materials had a purity of 99.99%. The Ti(OH)₄ precursor and commercially available Ba(OH)₂·8H₂O were added (Ti/Ba = 1:1 in molar ratio) into NaOH. After that, the mixture in a Teflon cup with 60% capacity was stirred and sealed tightly in a stainless steel autoclave. The closed bomb (Parr-type) [3] was maintained at the required temperature and time duration for hydrothermal reaction. The bomb was then cooled naturally to room temperature. The resulting white precipitate was washed extensively with DI water to remove any adsorbed impurities and finally dried at room temperature. The complete BaTiO₃ synthesis process is as follow:



4.2.1 Data and formula needed for calculating the amount of chemicals:

Density of NaOH	=	2.13g/cm ³
Molecular weight of NaOH	=	39.998g/mol
Molecular weight of Ti(OH) ₄	=	115.912g/mol
Molecular weight of Ba(OH) ₂ ·8H ₂ O	=	315.474g/mol
Volume of the Teflon container	=	43ml
Volume of the solvent	=	60% of Volume of the Teflon container
	=	25.8ml

Molarity	=	Moles of Solute/Volume of the Solvent(litre)
Moles	=	Mass(g)/Molecular Weight(g)
Volume	=	Mass(g)/Density(g/cm³ or g/ml)

4.2.2 Sample (S₁) :-

Ti(OH)₄ and Ba(OH)₂·8H₂O were added (Ti/Ba = 1:1 in molar ratio) into 0.25M of NaOH. For making the sample (S₁) of BaTiO₃ we have to calculate first the amount of these chemicals needed.

- Volume of solvent = 60% of Teflon cup
- The mass of 0.25M of NaOH for the given volume of solvent is calculated as:

Moles of NaOH = Molarity * Volume of Solvent
= 0.25 * (60% of the Volume of Teflon Container)
= 0.25 * (0.6 * 43/1000)
= 0.00645
Mass of NaOH = 0.00645 * 39.998
= 0.2579g

- The amount of Ti(OH)₄ and Ba(OH)₂.8H₂O required can be calculated as:

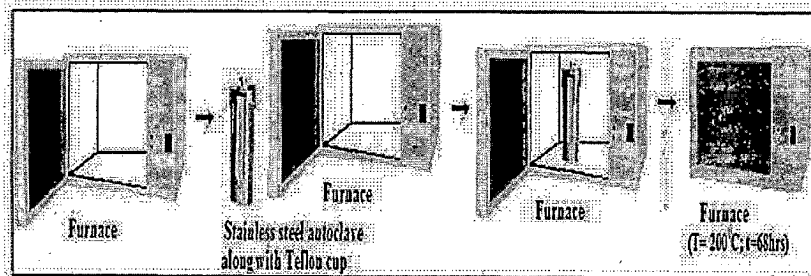
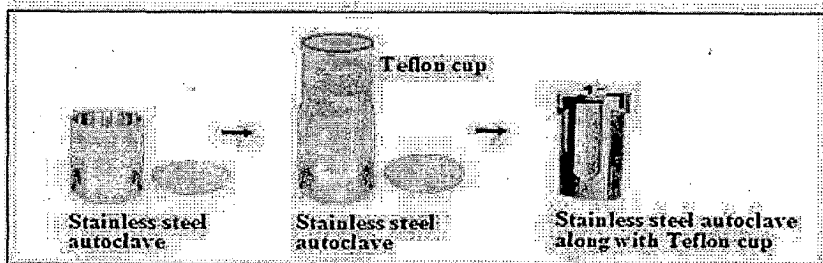
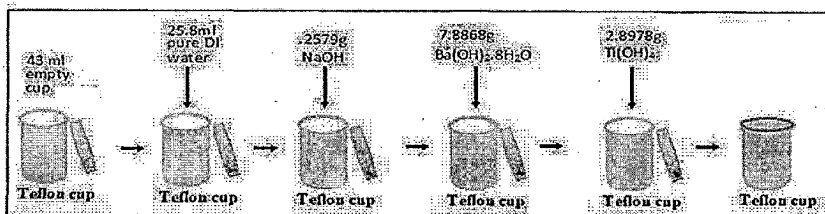
1mol of Ti(OH) ₄	=	115.912g
1mol of Ba(OH) ₂ .8H ₂ O	=	315.474g
For 1000ml		
Ti:Ba(molar ratio)	=	1:1
For 25ml		
Ti:Ba(molar ratio)	=	(115.912/40):315.474/40)
	=	(2.8978):(7.8868)
i.e		
Mass of Ti(OH) ₄	=	2.8978g
Mass of Ba(OH) ₂ .8H ₂ O	=	7.8868g

COMPOUND	AMOUNT	Constant/Variable
Water	25.8ml	Constant
Ba(OH) ₂ .8H ₂ O	7.8898g	Constant
Ti(OH) ₄	2.8978g	Variable
NaOH	0.2579g	Variable
Reaction temperature (T)	200 ⁰ C	Constant
Reaction time (t)	68hrs	Variable

Table 4.1 Parameters used for the synthesis of BaTiO₃ Sample (S₁)

After calculating the values of all the chemicals needed took the Teflon cup, add 25.8ml of water (60% of Teflon cup) in it. After that add 7.8868g of Ba(OH)₂.8H₂O in it followed by 2.8978g of Ti(OH)₄. Close the Teflon cup tightly and place it in a stainless steel autoclave. The complete container is placed in the furnace (oven) at 200⁰C for 68hrs. After the time period is elapsed, cool down the container at room temperature. Then put the white

precipitate formed into the beaker and washed it with DI water to remove the impurities and then dry it at room temperature to get the BaTiO₃ sample.



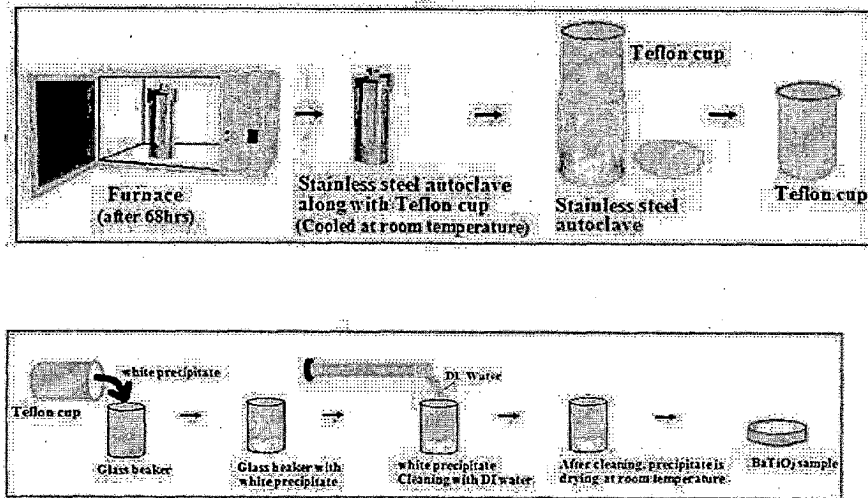


Figure 4.2 Complete layout of the hydrothermal process for BaTiO₃

The procedure for making the second (S₂) and third (S₃) sample is same as for the first sample. The only difference is in the amount of the Ti(OH)₄ and NaOH used for the reaction and the reaction time (t). By varying the amount of these chemicals we will check the change in fibre length and then calculate its effect on rate of H₂ production or PZEC efficiency.

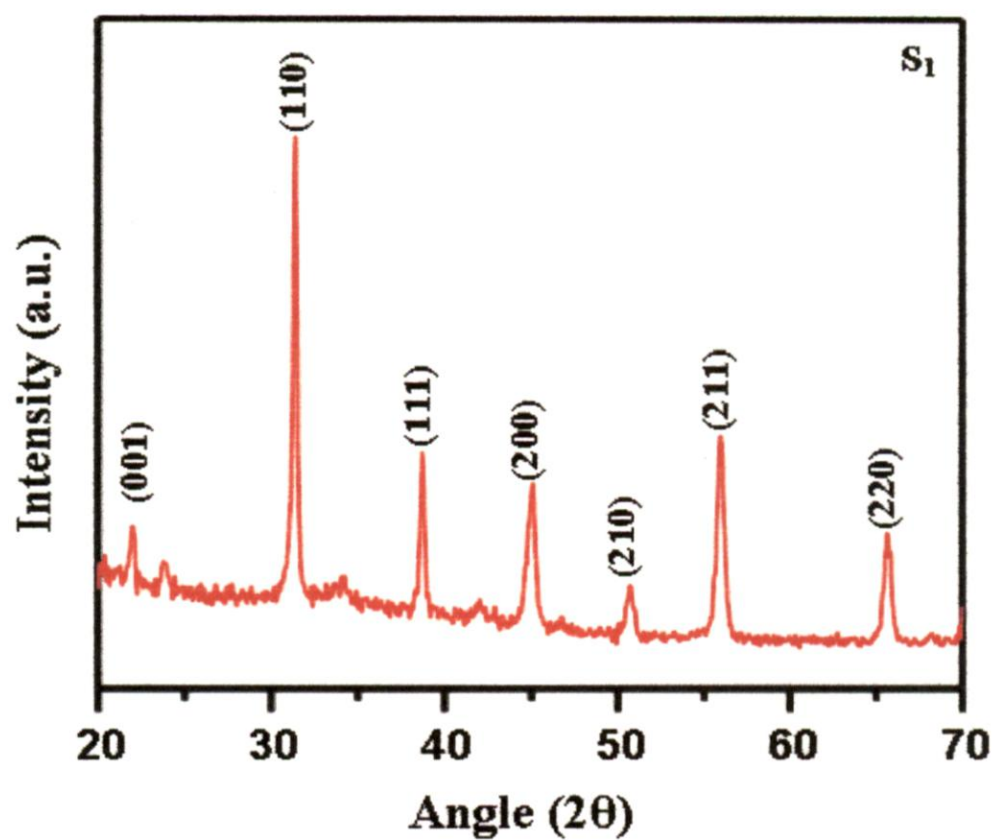


Figure 4.3 XRD image of BaTiO₃ sample (S₁)

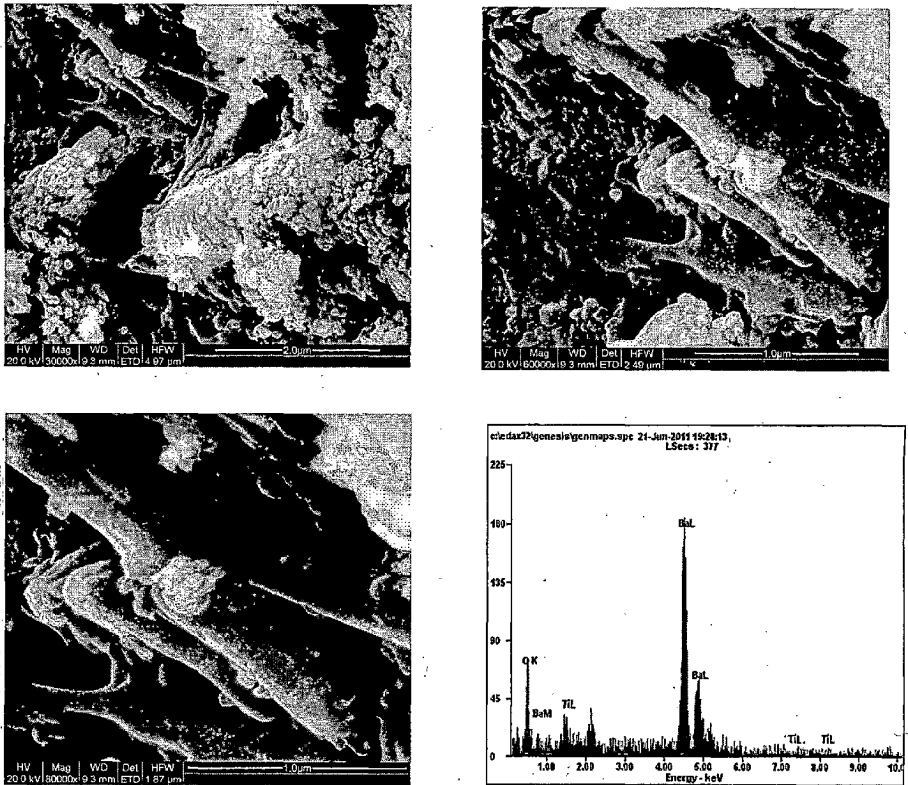
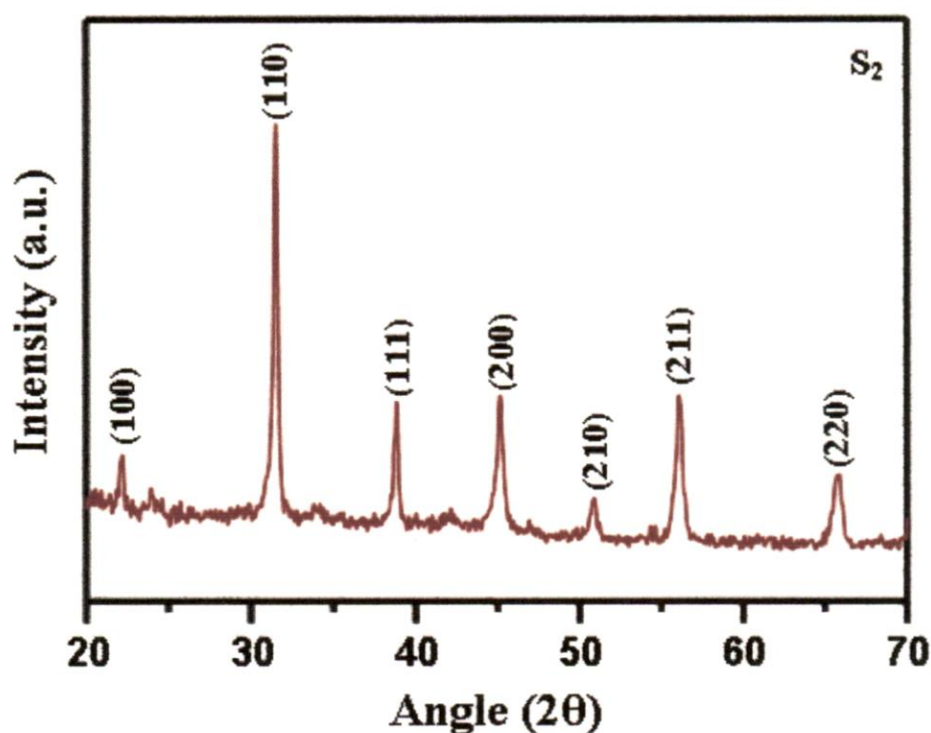


Figure 4.4 FE-SEM and EDS image of BaTiO₃ sample (S1)

4.2.3 Sample 2 (S₂) :-

COMPOUND	AMOUNT	Constant/Variable
Water	25.8ml	Constant
Ba(OH) ₂ .8H ₂ O	7.8898g	Constant
Ti(OH) ₄	2.9610g	Variable
NaOH	0.2670g	Variable
Reaction temperature (T)	200 ⁰ C	Constant
Reaction time (t)	96hrs	Variable

Table 4.2 Parameters used for the synthesis of BaTiO₃ Sample (S₂)Figure 4.5 XRD image of BaTiO₃ sample (S₂)

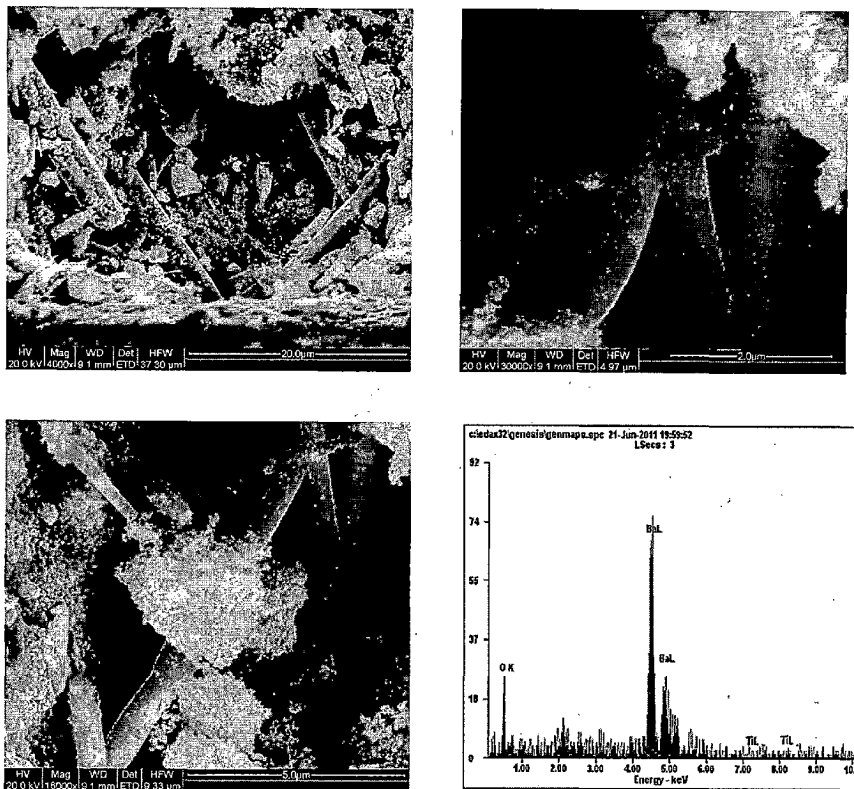
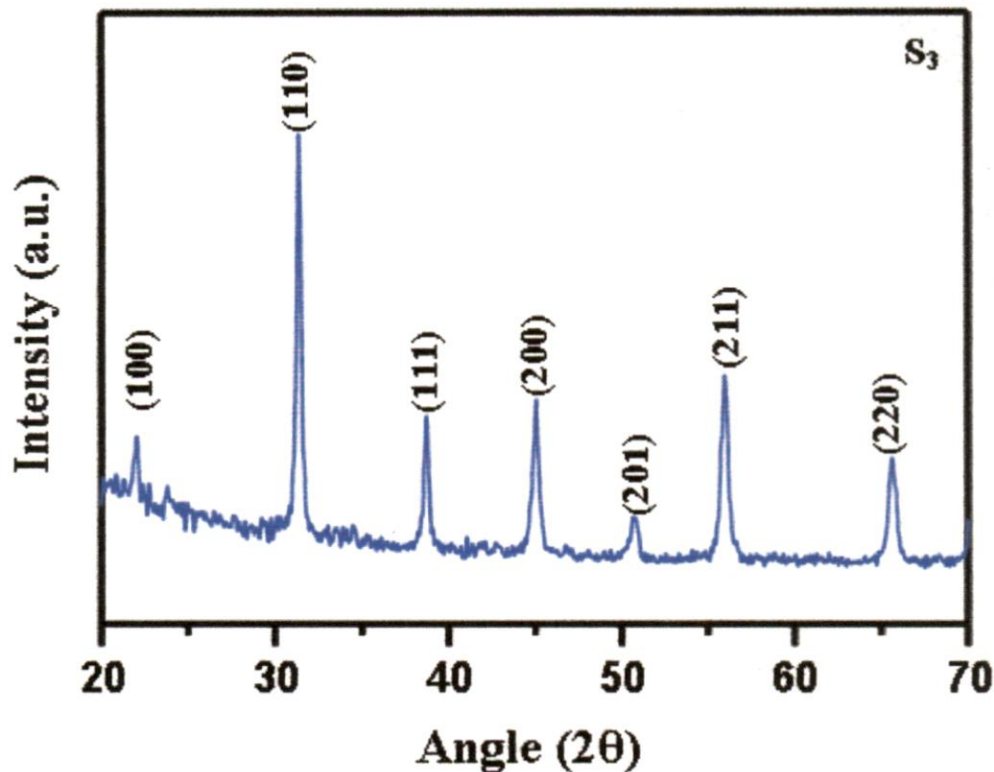


Figure 4.6 FE-SEM and EDS image of BaTiO₃ sample (S₂)

4.2.4 Sample 3 (S₃) :-

COMPOUND	AMOUNT	Constant/Variable
Water	25.8ml	Constant
Ba(OH) ₂ .8H ₂ O	7.8898g	Constant
Ti(OH) ₄	3.0620g	Variable
NaOH	0.2730g	Variable
Reaction temperature (T)	200 ^o C	Constant
Reaction time (t)	120hrs	Variable

Table 4.3 Parameters used for the synthesis of BaTiO₃ Sample (S₃)Figure 4.7 XRD image of BaTiO₃ sample (S₃)

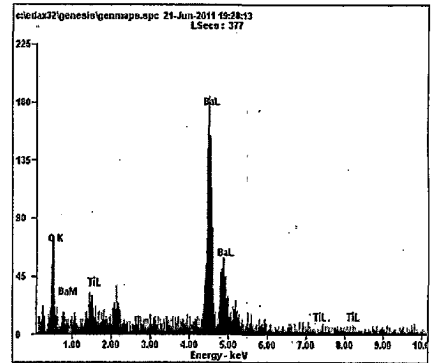
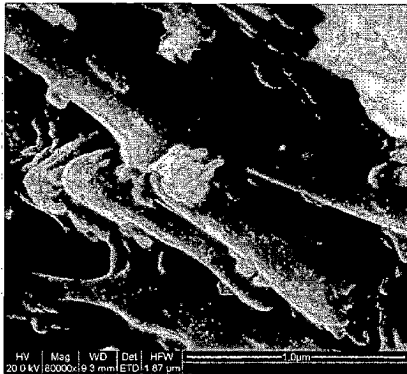
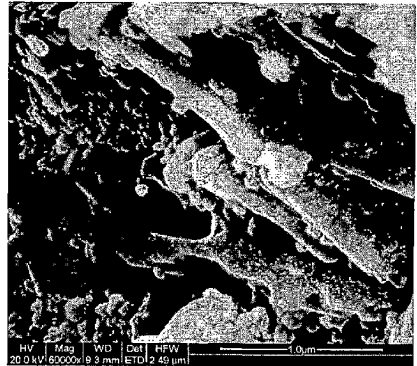
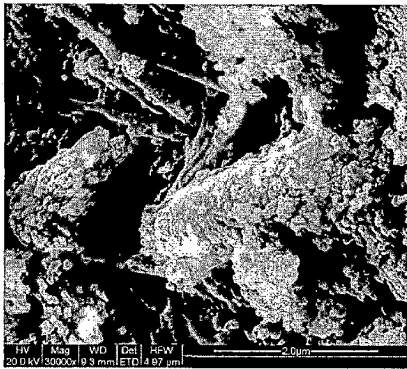


Figure 4.8 FE-SEM and EDS image of BaTiO₃ sample (S₃)

References

- [1] O'Donoghue, M. (1983). A guide to Man-made Gemstones. Great Britain: Van Nostrand Reinhold Company. pp. 40–44. ISBN 0-442-27253-7.
- [2] Laudise, R.A. (1986). "Hydrothermal Synthesis of Crystals". C&EN. September 28: 30–43.
- [3] "Hydrothermal Crystal Growth - Quartz". Roditi International. Retrieved 2006-11-17.
- [4] Spezzia, G. (1905). Accad. Sci. Torino Atti 40: 254.
- [5] Laudise, R.A. (1958). R.H. Doremus, B.W. Roberts and D. Turnbull, ed. Growth and perfection of crystals. Proceedings of an International Conference on Crystal Growth held at Cooperstown, New York on August 27–29, 1958.. Wiley, New York. pp. 458–463.



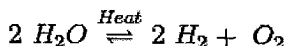
Chapter 5

*Direct Water Splitting
Process through Nano
crystals*

Handwritten text, possibly bleed-through from the reverse side of the page. The text is faint and difficult to decipher but appears to be organized into sections. The top section contains several lines of text, followed by a section starting with "Сторона 2" (Side 2). The bottom section contains a few more lines of text.

5.1 Water splitting process

Water splitting [1] is the general term for a chemical reaction in which water is separated into oxygen and hydrogen.



The decomposition of water (H_2O) into oxygen (O_2) and hydrogen gas (H_2) is due to the supply of energy in the form of heat, electricity etc. In this process chemically bonded elements and compounds are separated by passing an input energy more than the bond energy.

Production of hydrogen from water [2] is one of the important reasons for the water splitting processes. Hydrogen can be used to store renewable electricity when it is not needed (like the wind blowing at night) and then the hydrogen can be used to meet power needs during the day or fuel vehicles. This aspect helps make hydrogen an enabler of the wider use of renewables,^[2] and internal combustion engines.

Production of hydrogen requires large amounts of energy [3]. Usually, the input energy consumed for the hydrogen production is more valuable than the hydrogen produced so lots of methods have been discovered and testing in laboratories to find out the most efficient and economical way of hydrogen production.

Some of the important methods of water splitting [4] are:-

- Electrolysis
- Photoelectrochemical water splitting
- Photocatalytic water splitting

- Photobiological water splitting
- Thermal decomposition of water
- Chemical production
- Research

None of the “Research” methods of hydrogen production processes have been demonstrated at production levels, although several have been demonstrated in laboratories. One such research method of hydrogen production is explained experimentally in this chapter.

Process :-

The laboratory method of water splitting process through BaTiO₃ sample [5] is done by using ultrasonic waves (force). When external force is applied on BaTiO₃ fibres they will vibrate under its action and produces electric potential at the output with suitable adjustments.

The experiment of water splitting to hydrogen and oxygen was carried out using a sealed glass tube and samples in water under a standard condition. Glass tubes, 0.5 inch in diameter and 1 ft in length, were used for the experiment. The reaction cell (pyrex glass tube) was filled with nitrogen gas after adding the samples. Then ultrasonic wave vibrations using a Branson 5510-MT ultrasonic cleaner were applied to 5.0mL of DI water which results in production of hydrogen gas due to the piezoelectrochemical effect between the BaTiO₃ dendrites and water.

To monitor the hydrogen concentration variation, the gas inside of the cell was extracted by syringe and injected into an external hydrogen analyzer. The amount of hydrogen gas (H₂) produced from the water splitting experiment was monitored using an AMETEC Trace Analytical ta3000 gas chromatograph equipped with a reduction gas detector (RGD) sensor

for hydrogen detection. Nitrogen gas (N₂) of 99.998% purity at a flow rate of 20cc/min was applied as the carrier gas.

5.2 Experiment details :-

The following ingredients and equipments are used in the process:

- Ingredients :-
 - BaTiO₃ (sample)
 - DI water
 - Nitrogen gas
- Equipments :-
 - Pyrex Glass-tube
 - Rubber seal
 - Volumetric flask
 - Burette stand
 - Syringe
 - Vacuum pump
 - Ultrasonic cleaner
 - Gas chromatograph



Figure 5.1 Equipments used for the water splitting purposes

Pyrex glass tube is first cleaned with DI water and then dried. Now the amount of BaTiO_3 crystals needed is weighted on the digital weighing machine. After weighing the sample add it into the pyrex tube.

The volume of DI water to be added is first measured with the volumetric flask and then poured into the tube. After adding the sample and water to the tube close it with the rubber stopper.

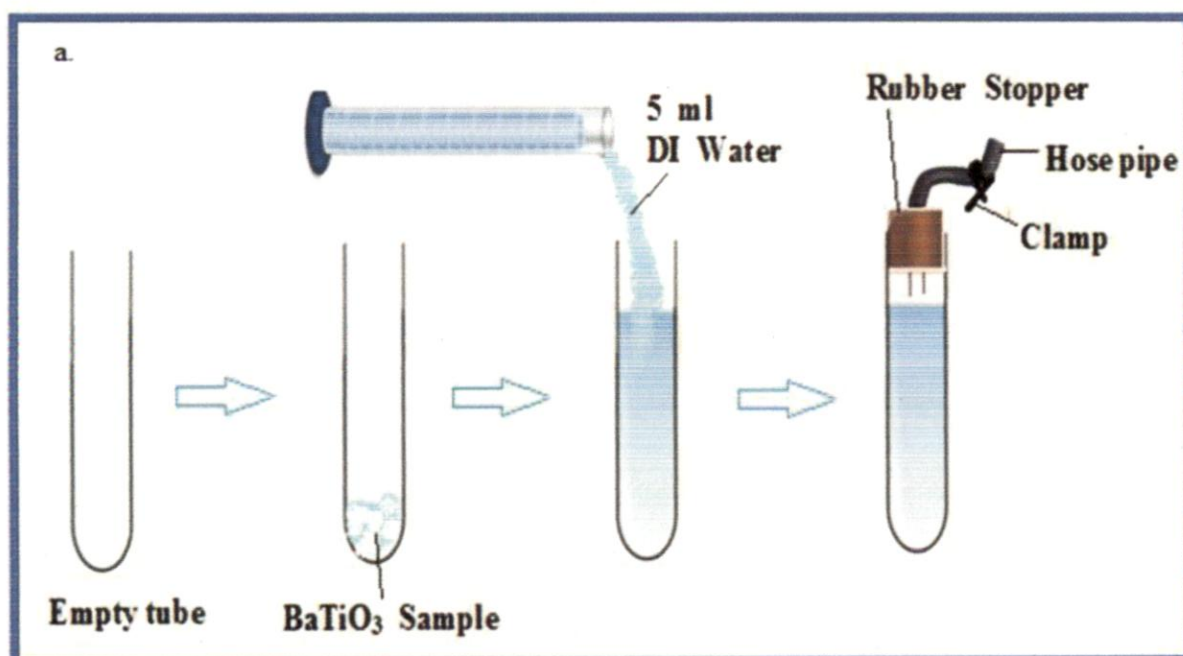
Rubber stopper is provided with a hose pipe and a clamp to loose or fasten it as per the requirement. Now the sealed glass tube has to be evacuated or vacuumed so that we can add the nitrogen (N_2) gas in it. Vacuum is created inside the rubber sealed tube by using a vacuum pump.

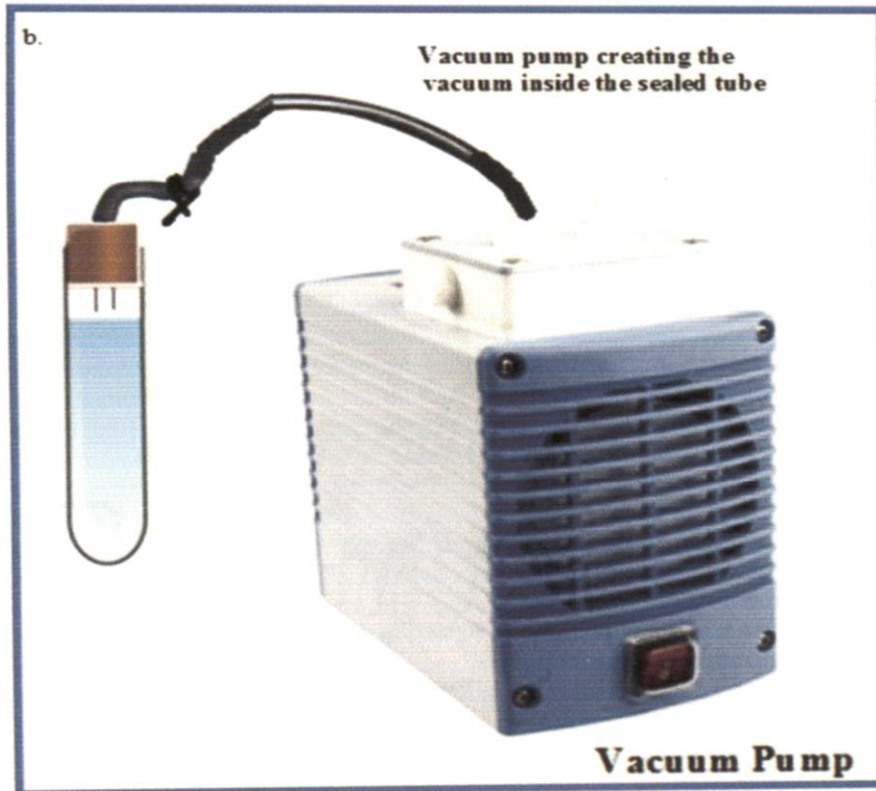
Now the vacuumed tube is connected with the nitrogen gas cylinder to create an inert atmosphere of nitrogen inside the tube. When the nitrogen gas is filled completely inside the tube, sealed the tube with the help of clamp.

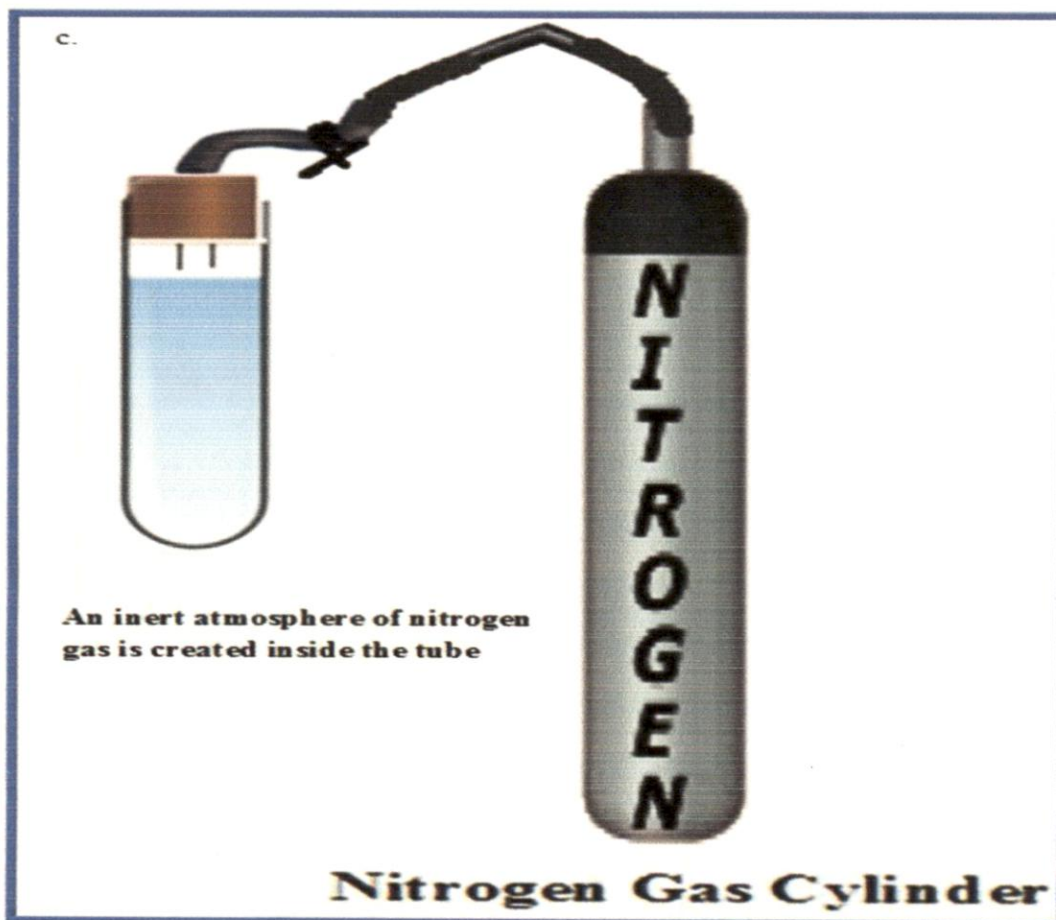
The sealed tube is fitted in the burette stand and placed in the ultrasonic bath. The depth of the tube in the ultrasonic bath should be such that it will completely dip the sample inside the bath. The vibration generated by the ultrasonic waves acts as an external force on the piezo material and it will generate a potential at its outlet. Since the material is in direct contact with the water the energy generated at the sample outlet is utilized by water for the splitting process if the potential developed is more than 1.23eV.

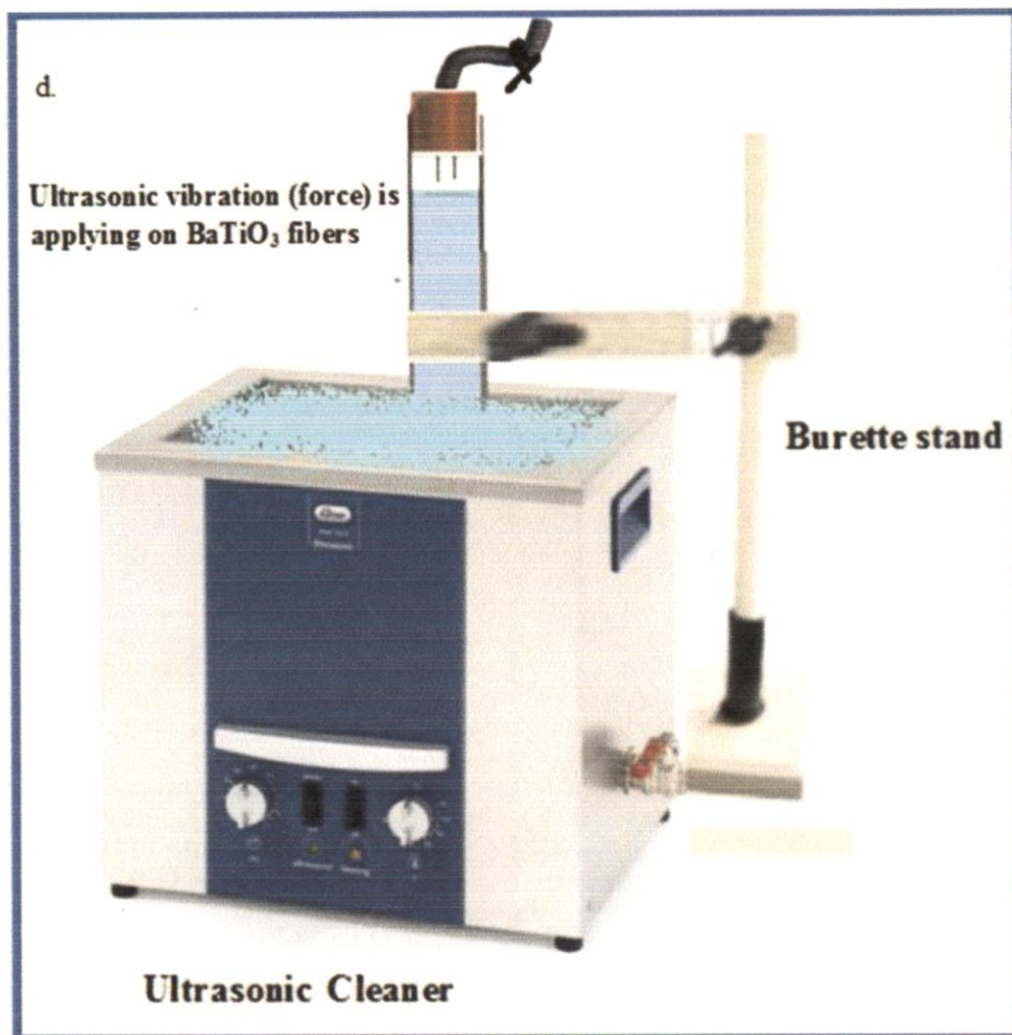
BaTiO ₃ (Sample) mass	= 0.5g
DI water volume	= 5ml
Time duration for vacuum process	= 10mins
N ₂ gas supply time	= 10mins
Ultrasonic wave frequency used	= 40kHz
Ultrasonic vibration time duration	= 1hrs

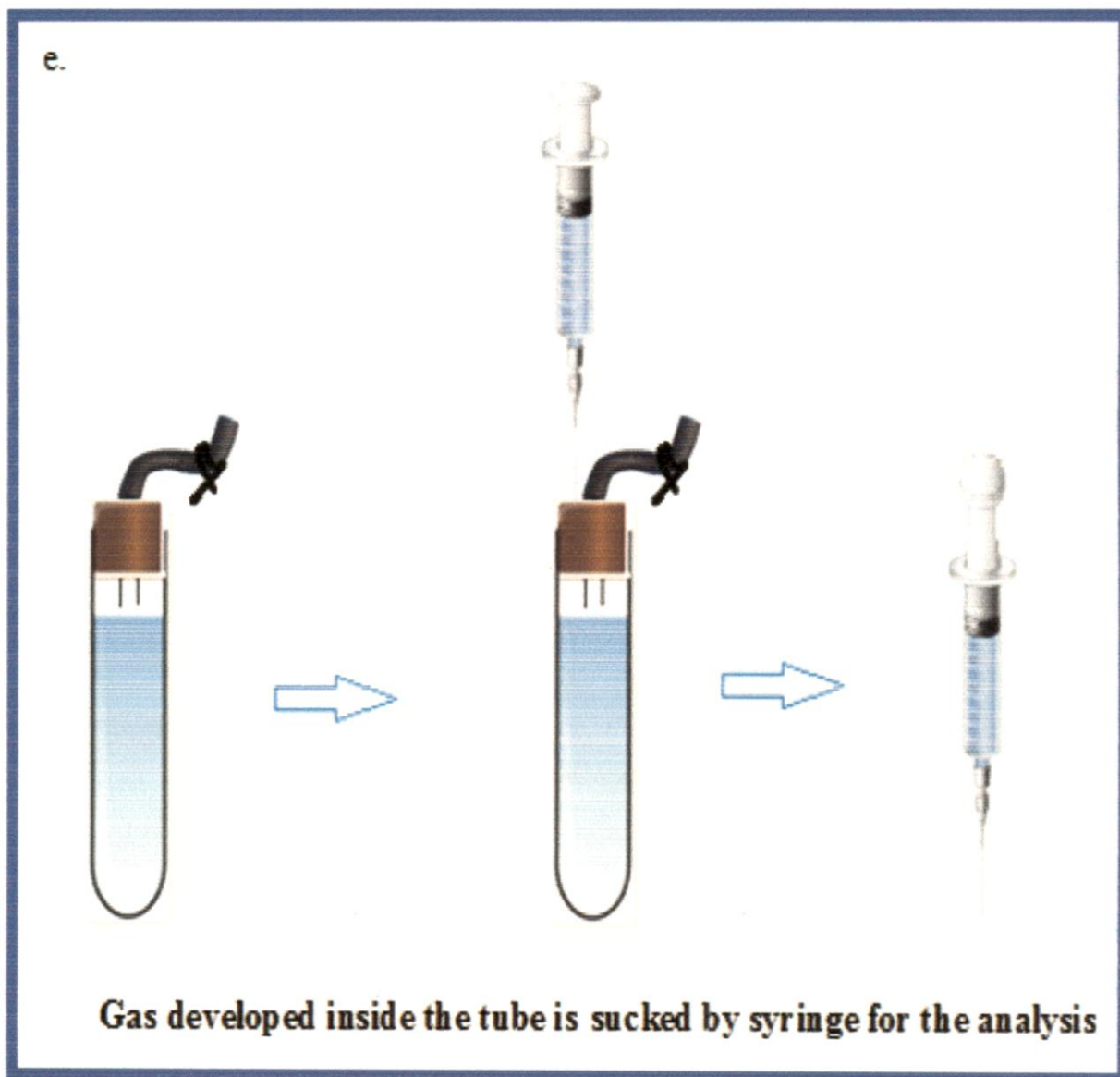
After the PZEC (piezoelectrochemical) reaction over, suck the gas collected inside the tube with the help of syringe and inject it in the gas chromatograph. The quantitative and qualitative detection of the gases produced, are analysed in the gas chromatograph.

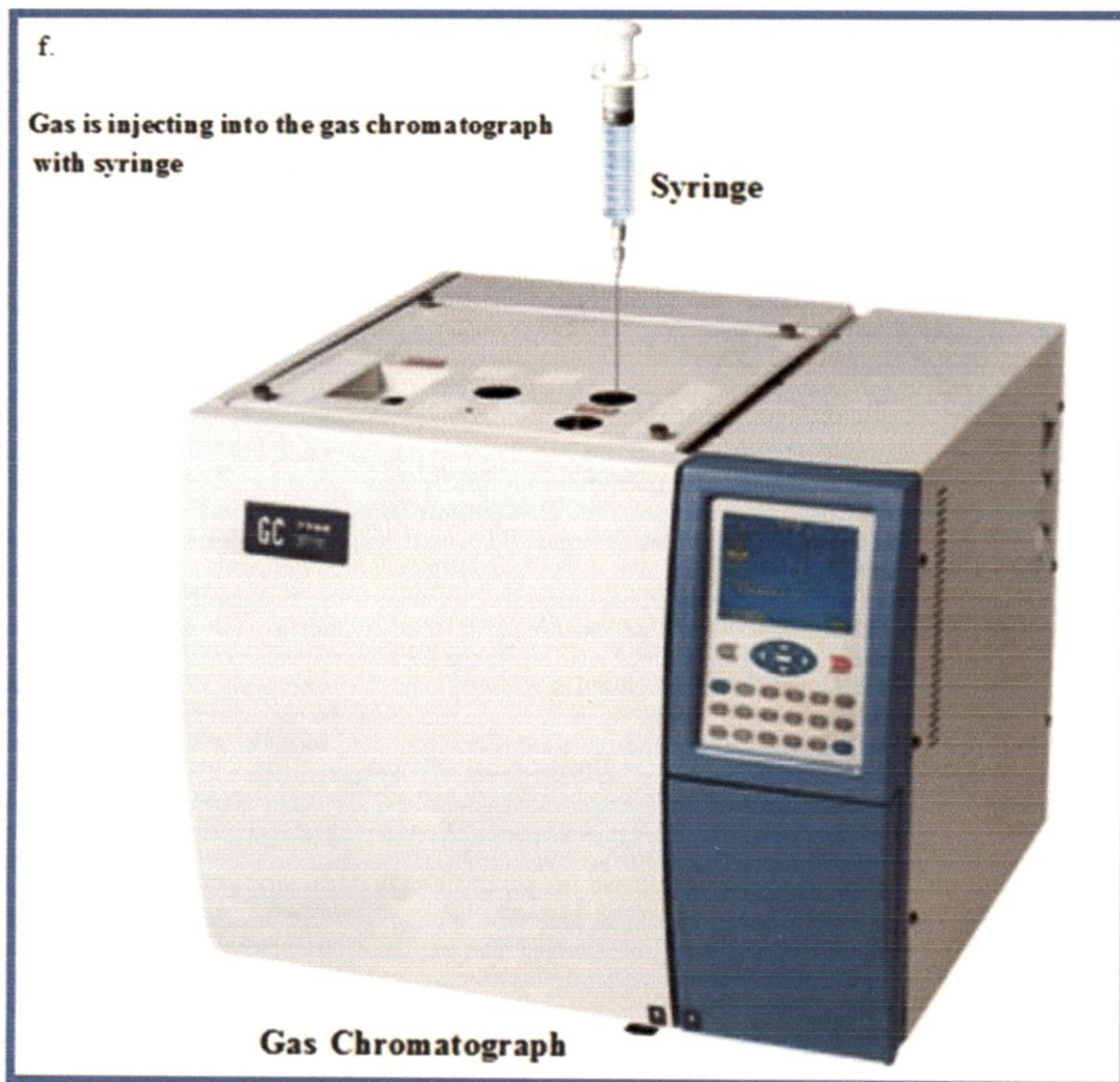












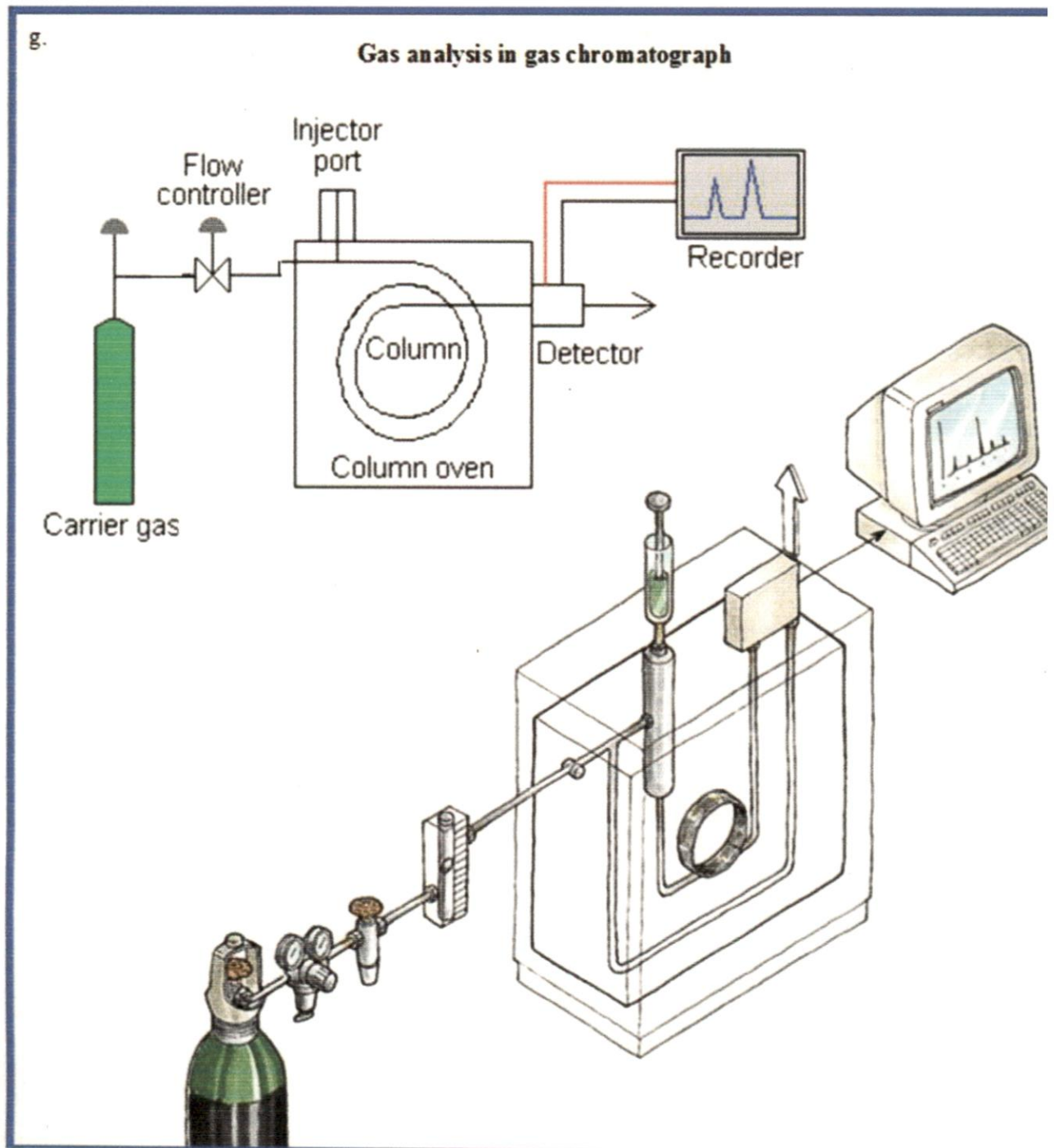
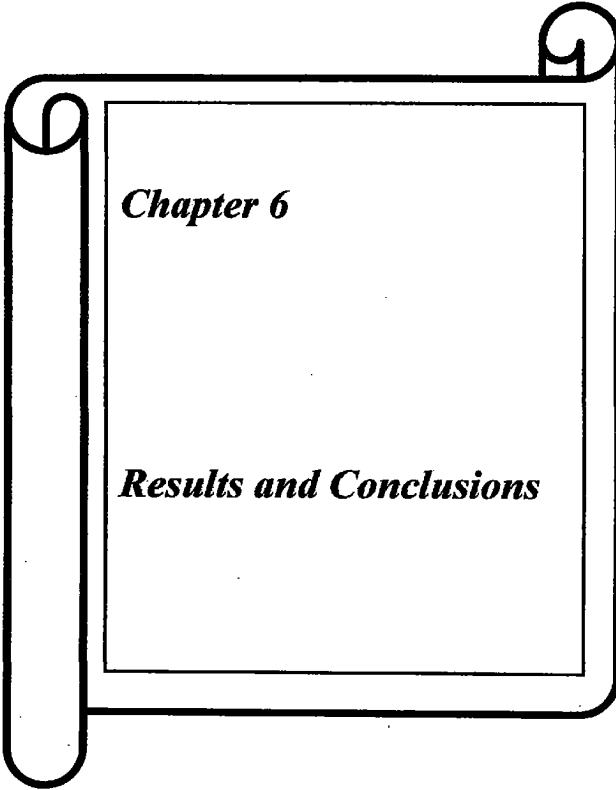


Figure 5.2(a, b, c, d, e, f) Layout of complete water splitting process and gas detection technique

References

- [1] Del Valle, F.; Ishikawa, A.; Domen, K.; Villoria De La Mano, J.A.; Sánchez-Sánchez, M.C.; González, I.D.; Herreras, S.; Mota, N. et al. (May 2009). "Influence of Zn concentration in the activity of Cd_{1-x}Zn_xS solid solutions for water splitting under visible light". *Catalysis Today (ScienceDirect)* **143** (1-2): 51–59.
- [2] Del Valle, F. et al; Álvarez Galván, M. Consuelo; Del Valle, F.; Villoria De La Mano, José A.; Fierro, José L. G. (Jun 2009). "Water Splitting on Semiconductor Catalysts under Visible-Light Irradiation". *Chemsuschem (CHEMSUSCHEM)* **2** (6): 471–485.
- [3] Del Valle, F. et al; Del Valle, F.; Villoria De La Mano, J.A.; Álvarez-Galván, M.C.; Fierro, J.L.G. (2009). "Photocatalytic water splitting under visible Light: concept and materials requirements". *Advances in Chemical Engineering (ScienceDirect)* **36**: 111–143
- [4] Belitskus, David (August 1970). "Reaction of Aluminum with Sodium Hydroxide Solution as a Source of Hydrogen" (PDF). *Journal of the Electrochemical Society* (Pennington, New Jersey: ECS) **117** (8): 1097–1099.
- [5] Soler, Lluís; Macanás, Jorge; Muñoz, Maria; Casado, Juan (2007). "Synergistic hydrogen generation from aluminum, aluminum alloys and sodium borohydride in aqueous solutions". *International Journal of Hydrogen Energy (Elsevier)* **32** (18): 4702–4710.



Chapter 6

Results and Conclusions

Surface morphology of BaTiO₃ has been studied by XRD and FE-SEM.

6.1 XRD Data

XRD data reveals that BaTiO₃ formed by hydrothermal method is polycrystalline in nature having (110) preferred orientation. We find from our XRD data that intensity of (110) main peak increase with the increase in time duration, from 72 hour to 120 hour for the fabrication of BaTiO₃, and hence the particle size has been greatly increased for S₃ sample.

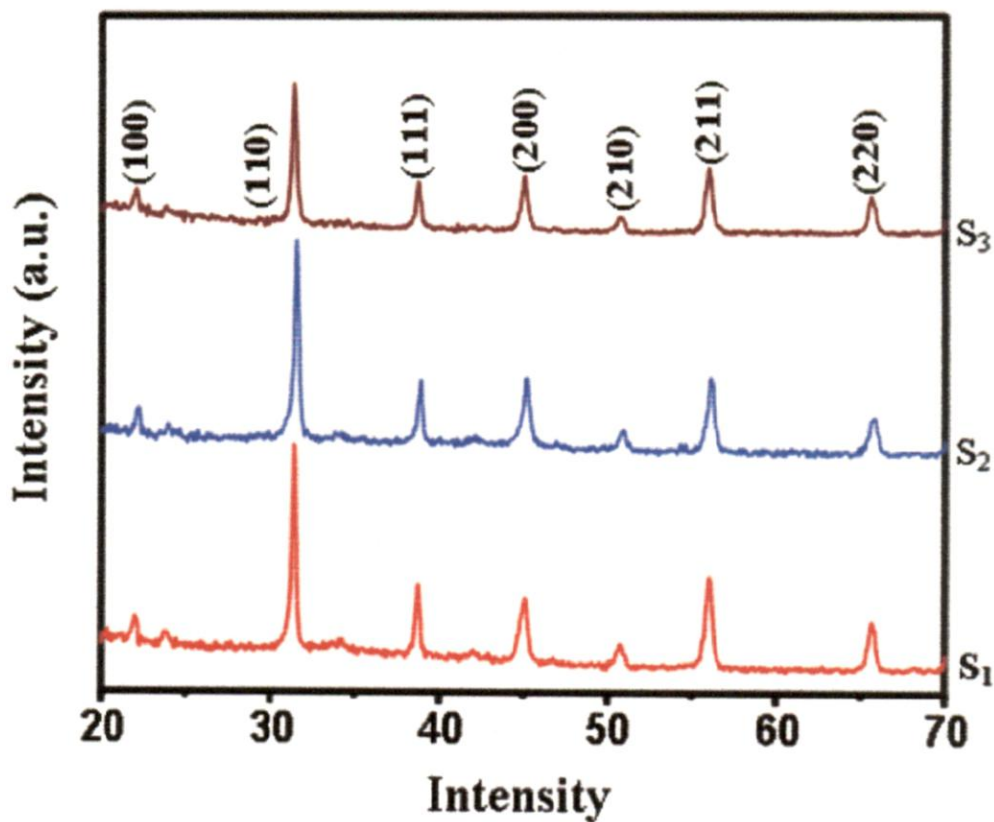


Figure 6.1 XRD image for BaTiO₃ samples S₁, S₂ and S₃

Also with the increase in time duration, intensity of other peaks decreases, figure (6.1), it means that on increasing the time duration crystallinity of BaTiO₃ has been increased. A particle size of BaTiO₃ has been calculated from scherr formula.

$$\text{Particle size} = \frac{0.9 \lambda}{\beta \cos \theta}$$

where β is F.W.H.M*

Sample	β (110)	Particle size (110) nm
S ₁	0.14929	54
S ₂	0.1387	58
S ₃	0.1195	68

*Full width at half maxima

Table 6.1 XRD data for BaTiO₃ samples S₁, S₂ and S₃

6.2 FE-SEM Data

Figure (6.2) shows the FE-SEM images, from these images we found that perovskite BaTiO₃ form dendrite structure. The length of these fibers has been calculated from FE-SEM Images and listed in table (6.2). From these we found that fiber length has been increased manifold.

Sample	Fibre length (μm) approx value
S ₁	3
S ₂	7
S ₃	9

Table 6.2 Fibre length of BaTiO₃ samples S₁, S₂ and S₃

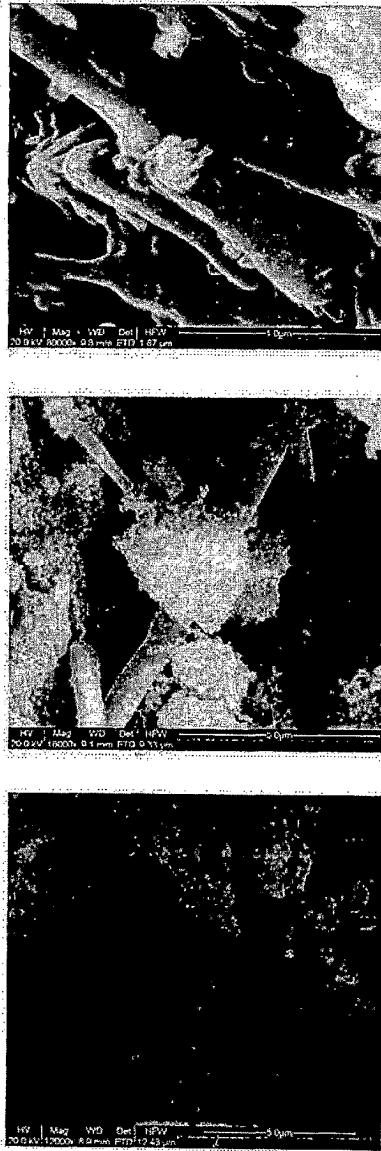


Figure 6.2 FE-SEM images of BaTiO₃ samples S₁, S₂ and S₃ respectively



Chapter 6

Results and Conclusions

In recent years, photocatalytic water splitting using oxide semiconductors under irradiation has received great attention. However, the number of available photocatalysts is currently limited, and their performance is hampered by their effectiveness, efficiency, and usage life. The demand for new mechanisms of direct water splitting to yield greater energy efficiency is rapidly increasing. In this study, we report the direct conversion of mechanical energy to chemical energy; termed the piezoelectrochemical (PZEC) effect. The mechanism of the water decomposition via the PZEC effect relies on the piezoelectric properties of the materials.

Tetragonal BaTiO_3 structure display unique piezoelectric properties. With this property as discussed in the report we are able to split the water in Hydrogen and oxygen. Since hydrogen is the source of huge amount of energy and with the production of hydrogen we can solve the world's energy deficit problem to a large extent.

Utilization of hydrogen energy has many attractive features, including energy renewability, flexibility, and zero greenhouse gas emissions. If we will be able to generate hydrogen fuel at commercial/Industrial level by using this method of water splitting, then this will be a simple and cost-effective technology to generate hydrogen fuels.

Below in the figure (7.1) we have try to show how hydrogen can be used as a fuel in automobile with self-hydrogen generating system using piezoelectric materials.

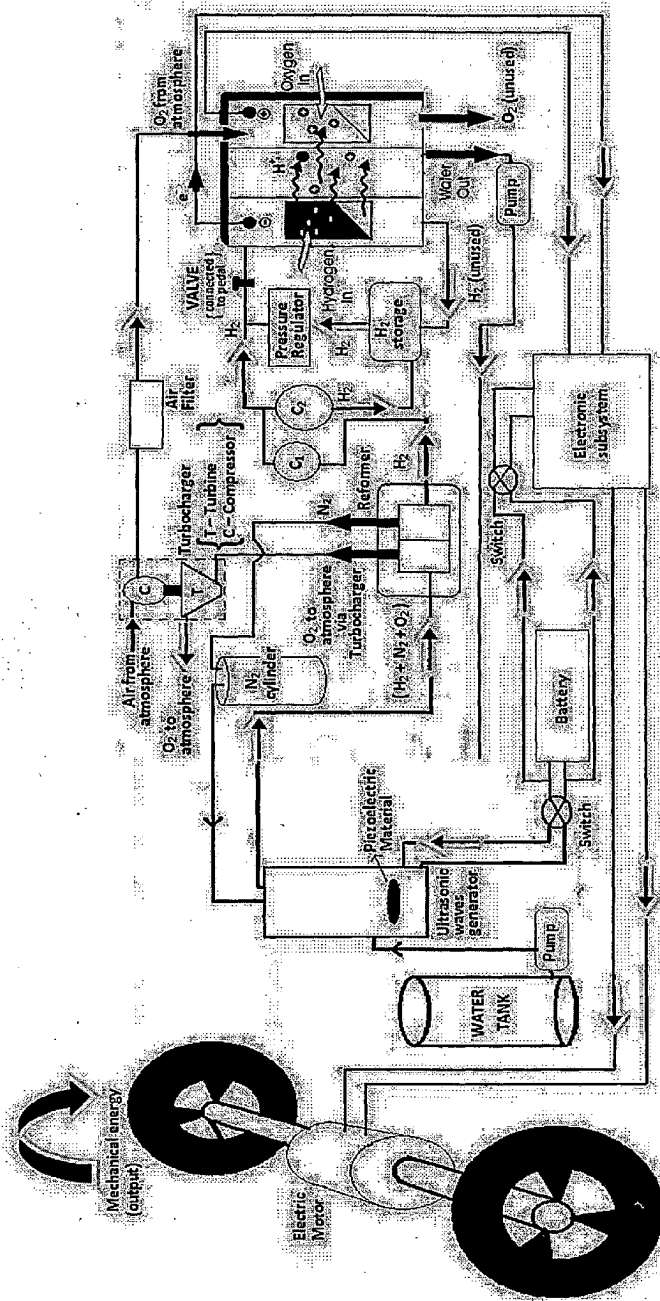


Figure 7.1 Future application in the field of automobiles — Self-hydrogen generation vehicles

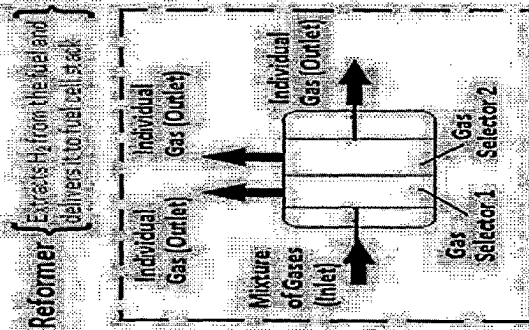
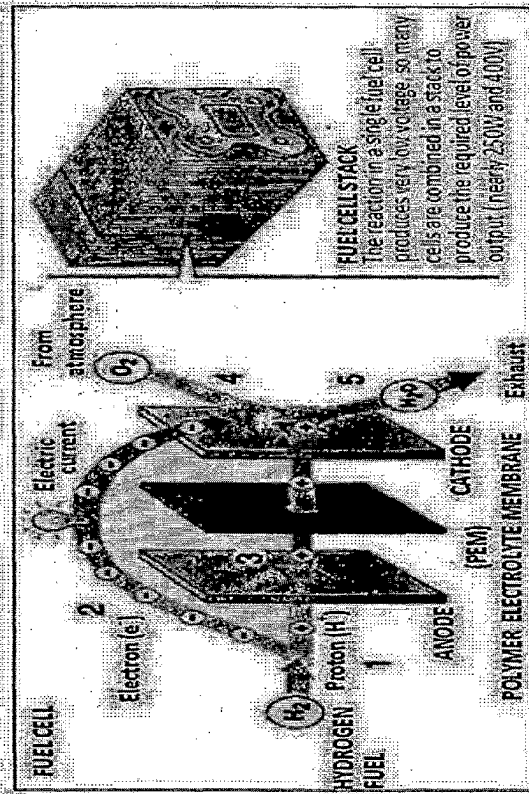


Figure 7.2 Detail description of some parts of self-hydrogen generation vehicle